Electronic Supplementary Material (ESI) for CrystEngComm.


# Synthesis, structures and properties of metal-organic frameworks prepared using a semi-rigid tricarboxylate linker

Daniel Rixson, Güneş Günay Sezer, Emre Alp, Mary F. Mahon and Andrew D. Burrows

**Electronic supplementary information**

## 1. General experimental procedures

### *1.1 Powder X-ray Diffraction*

Powder X-ray diffraction (PXRD) patterns were recorded on either a Bruker AXS D8 Advance diffractometer using copper $K_\alpha$ radiation (λ = 1.5406 Å) at 298 K or on a STOE Powder Diffraction System in using copper $K_\alpha$ radiation (λ = 1.540589 Å) at 298 K. On the D8 the beam slit was set to 1 mm, detector slit to 0.2 mm and anti-scattering slit set to 1 mm. Samples were dried on a filter paper prior to the measurement and then ground on to the mounted slide using a second slide. Data was collected between 5-60° with a step size of 0.024° and a scan speed of 0.3 s/step. On the STOE instrument patterns were collected in transmission mode using a multi-MYTHEN detector with a step size if 0.015° and 600 secs/step (detector). Samples were dried on a filter paper prior to the measurement and then ground using a pestle and mortar. The powder was immobilised between two acetate sheets in the sample holder with the aid of resin/IPA based glue if necessary.

### *1.2 Spectroscopy*

Nuclear Magnetic Spectroscopy was carried out at 298 K on either a Bruker Advance 300 MHz Ultrashield NMR spectrometer or an Agilent 500 MHz NMR spectrometer. All peaks were referenced to residual proton peaks from the solvent. FTIR spectroscopy was carried out on solid samples using a Perkin Elmer Spectrum 100 spectrometer mounted on a diamond/gem platform.

### *1.3 Thermogravimetric analysis (TGA)*

TGA was conducted using a Setsys Evolution TGA 16/18. Once the instrument has been calibrated, a small, powdered sample (5 – 20 mg) was put into a 170 µL aluminium crucible which was placed onto the internal instrument balance. The sample was then subject to a pre-programmed heating profile of 10 °C/min under a flow of air.

### *1.4 Microanalyses*

Elemental analysis was conducted by either London Metropolitan University or Exeter Analytical UK Ltd.

## 2. Synthesis and characterisation

MOF syntheses were carried out in microwave reaction tubes (10 mL or 30 mL) and sealed with a Teflon lined cap. Where higher pressures are generated Parr acid digestion bombs were utilised. In general, the synthesised materials were stored under solvent to maintain pore solvent content and crystallinity. All reported materials were synthesised in good yields (40%-90%), exact values are not given due to the ambiguity of pore solvent and the need to keep the material under solvent.

*2.1 Synthesis of 5-((carboxymethyl)amino)isophthalic acid ($H_3$cmai)*

5-Aminoisophthalic acid (25 mmol, 4.53 g) was dissolved in MeOH (150 mL). To this solution was added glyoxalic acid monohydrate (30 mmol, 2.76 g). The reaction mixture was stirred at room temperature for 5 hours after which $NaCNBH_3$ (32 mmol, 2.01 g) was added in one portion. The reaction mixture was left stirring at room temperature overnight in which time an off-white product had precipitated. This was collected by vacuum filtration and dried in an oven for 6 hours. (Yield 4.27 g, 71%). The identity of the product was confirmed via $^1$H-NMR (500 MHz, DMSO-$d_6$); δ (ppm) 7.68 (1H, s), 7.23 (2H, s), 3.56 (2H, s) and $^{13}$C-NMR (125.7 MHz, DMSO-$d_6$); δ (ppm) 173.1, 168.8, 148.7, 134.3, 118.4, 116.3, 46.7. The $^1$H NMR and $^{13}$C{$^1$H} NMR spectra are shown in Figures S1 and S2 respectively.

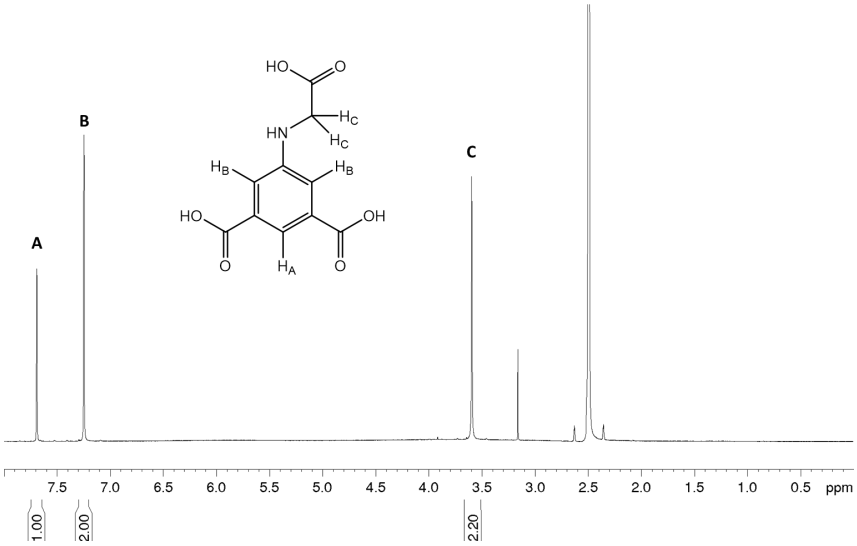


**Figure S1.** $^1$H-NMR spectrum of $H_3$cmai in DMSO-$d_6$.

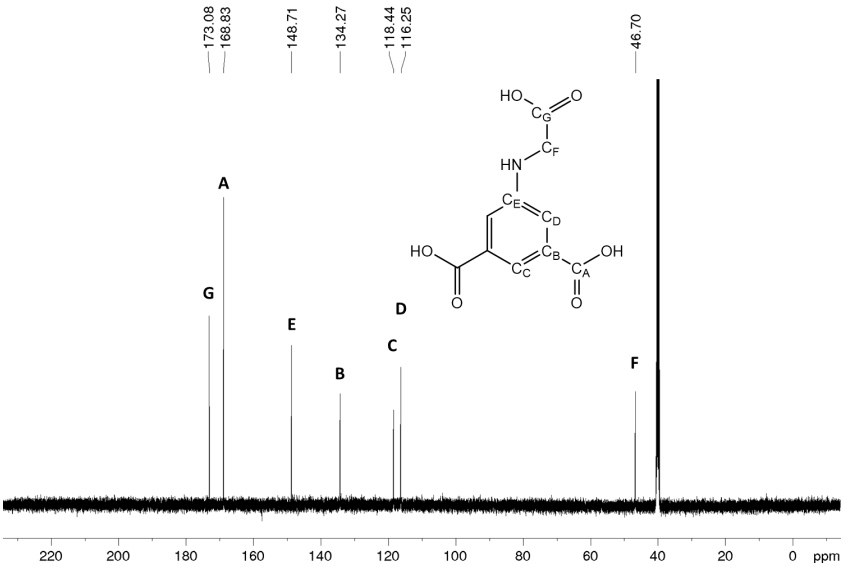


**Figure S2.** $^{13}$C-NMR spectrum of $H_3$cmai in DMSO-$d_6$.

### *2.2 Synthesis of [$Cd_2(Hcmai)_2(H_2O)_2$]·$H_2O$ (**1**)*

$Cd(NO_3)_2 \cdot 4H_2O$ (1 mmol, 0.3085 g) and $H_3$cmai (0.3 mmol, 0.0717 g) were placed in a 30 mL microwave reaction vessel. 18 mL of deionised water was added, and the mixture magnetically stirred for 15 minutes after which it was sealed with a Teflon lined cap and placed in an oven at 90 °C for three days. After cooling large light brown plate crystals were collected via vacuum filtration, washed with deionised water and stored in fresh deionised water until required.

The experimental PXRD pattern for compound **1** shows reasonable agreement with the simulated pattern (Figure S3), intensity discrepancies between the patterns can be attributed to preferred orientation. There are also a few peaks which do not match suggesting a second phase may be present.

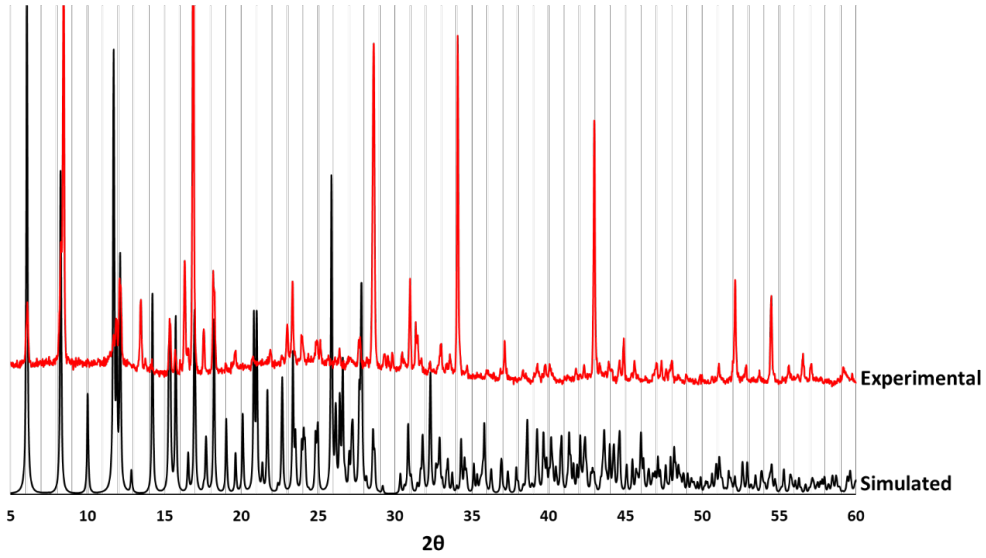


**Figure S3.** Comparison of simulated and experimental PXRD for compound **1**.

Thermogravimetric analysis was carried out on compound **1**, with the results presented in Figure S4. A mass loss between 30 and 195 °C of 7.30%, matches well with the theoretical loss of 7.18% for 3 water molecules. After 195 °C, there is a sharp drop in mass, which is attributed to the breakdown of the framework.

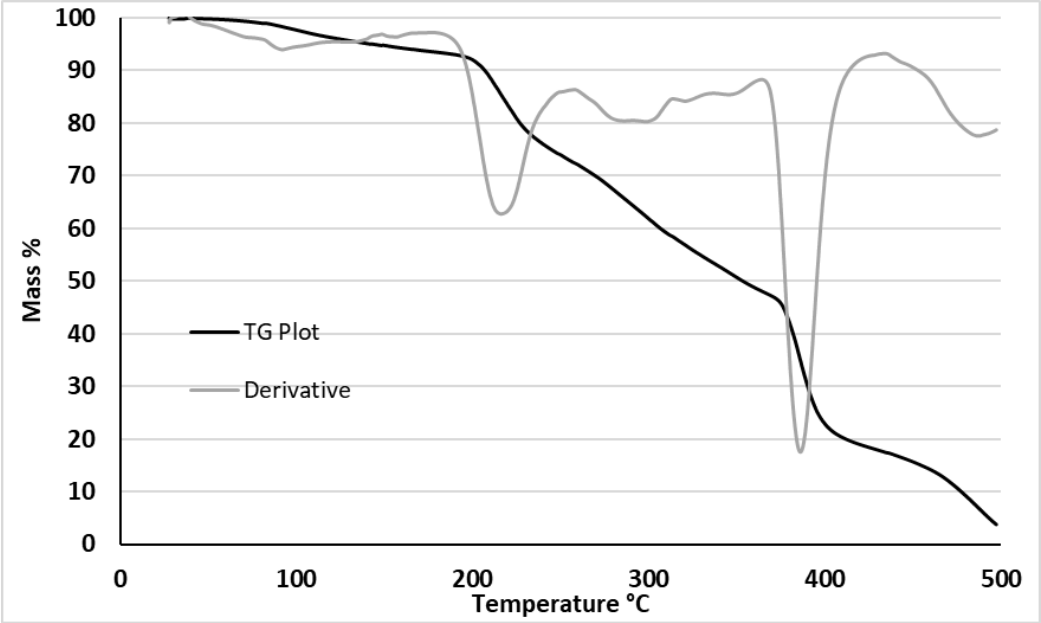


**Figure S4.** Thermogravimetric analysis of compound **1**.

The IR spectrum of compound **1** is shown in Figure S5: (solid, $cm^{-1}$) 3306s (br), 3260w, 1706w, 1680w, 1602m (sh), 1540s, 1420s, 1398s, 1301s, 1228s, 948m, 924m, 763s, 678s.

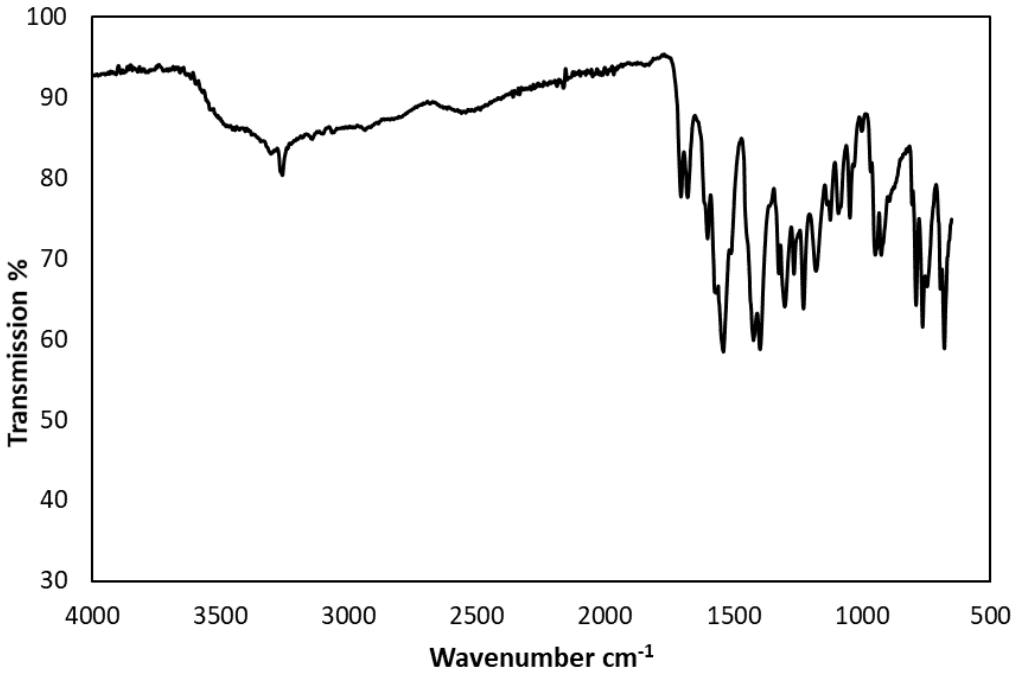


**Figure S5.** Infrared spectrum of compound **1**.

### *2.3 Synthesis of [Cd(Hcmai)($H_2O$)$_2$] (**2**)*

$CdCl_2 \cdot 2.5H_2O$ (0.6 mmol, 0.1370 g) and $H_3$cmai (0.2 mmol, 0.0478 g) were put into to a 10 mL microwave vial containing 8 mL of $H_2O$ and sonicated for 15 minutes. The vial was then placed in an oven for three days at 90 °C. After cooling to room temperature, the intergrown brown blocks were collected using vacuum filtration, washed with deionised water and stored in fresh deionised water until required.

The experimental PXRD pattern for compound **2** shows good agreement with the simulated pattern (Figure S6), the discrepancy in the intensities of the patterns can be attributed to preferred orientation, with the extra peaks suggesting the presence of a minor second phase. Elemental microanalysis (CHN) was also carried out and showed good agreement in with the theoretical values based on the solved structure for compound **2**. Expected based on crystal structure: C 31.15%, H 2.88%, N 3.63%. Found: C 31.02%, H 2.77%, N 3.43%.

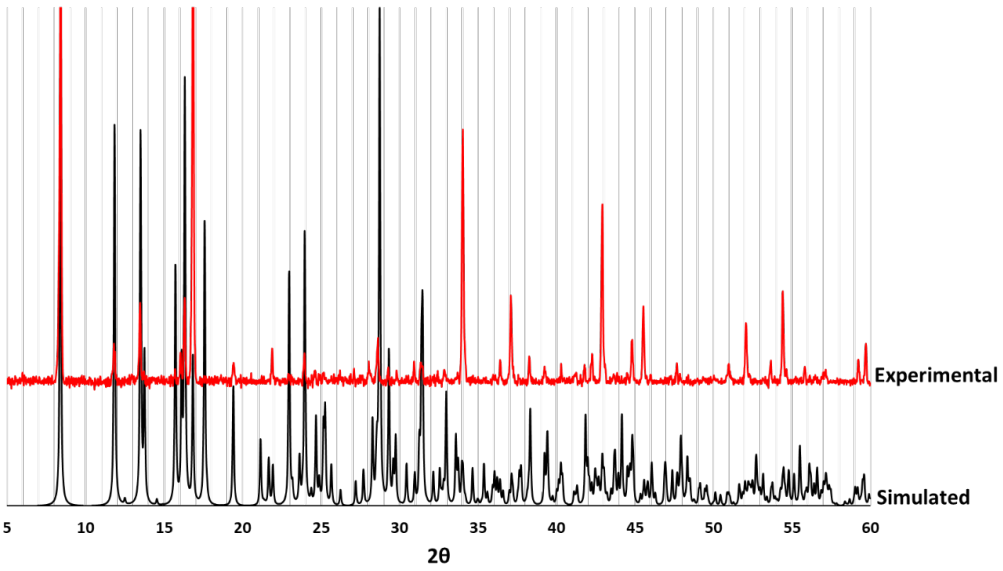


**Figure S6.** Comparison of simulated and experimental PXRD for compound **2**.

Thermogravimetric analysis was carried out on compound **2** and the results are presented in Figure S7. The mass loss between 175-220 °C was 7.53%. The loss of the two ligated water molecules from the structure would give a mass loss of 9.35% so the observed mass loss is slightly lower than expected in this region, possibly due to the presence of a second phase.

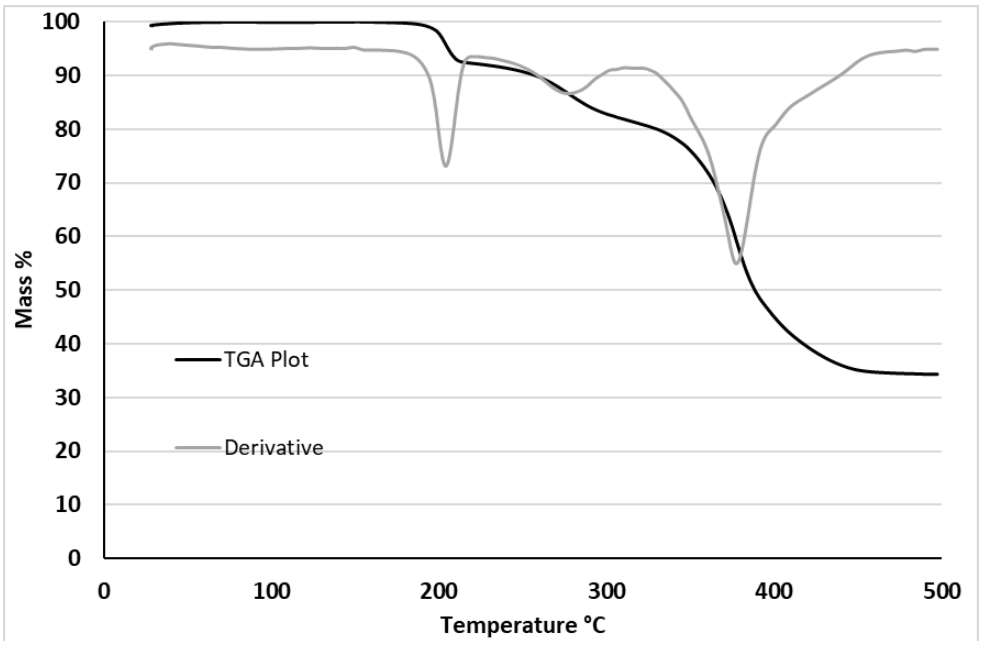


**Figure S7.** Thermogravimetric analysis of compound **2**.

The IR spectrum of compound **2** is shown in Figure S8: (solid, $cm^{-1}$) 3243w, 3030s (br), 1693w, 1590m, 1542s, 1402s, 1246s, 1198s, 942s, 765s, 677s.

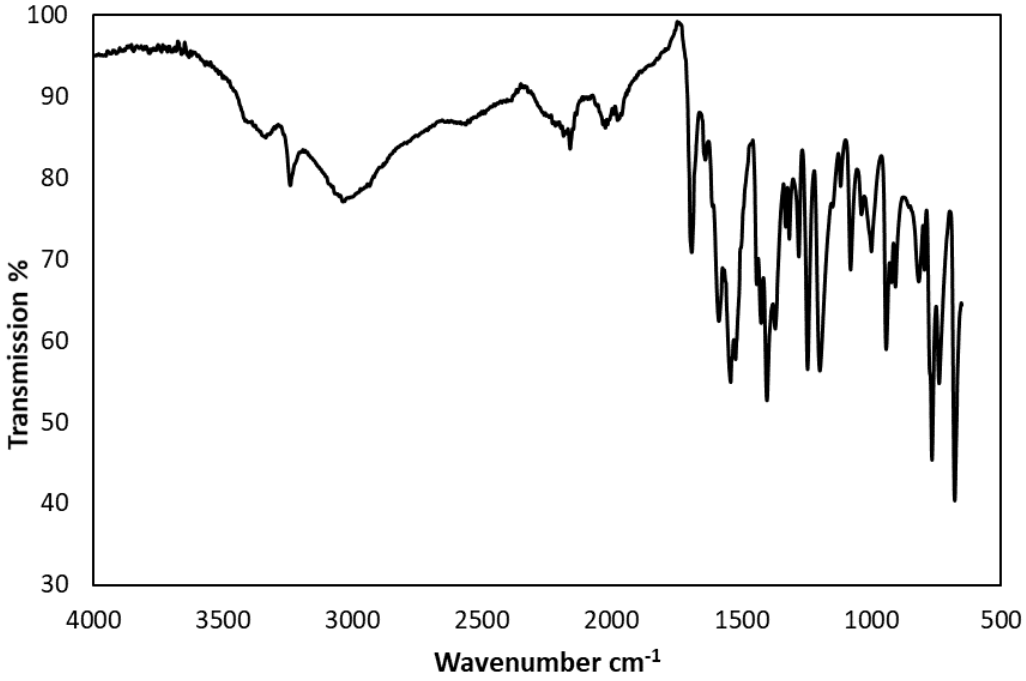


**Figure S8.** Infrared spectrum of compound **2**.

### *2.4 Synthesis of $[Cd_3(cmai)_2(H_2O)_2]\cdot 4H_2O$ (**3**)*

$Cd(OAc)_2\cdot 2H_2O$ (0.6 mmol, 0.1599 g) and $H_3$cmai (0.2 mmol, 0.0478 g) were placed in a 10 mL microwave vial containing 9 mL of $H_2O$ and sonicated for 15 minutes. The vial was sealed and then placed in an oven at 90 °C for three days. After cooling to room temperature, the colourless rhombohedral block shaped crystals were collected by vacuum filtration and washed with deionised water and stored in fresh deionised water until required.

The simulated and experimental patterns (Figure S9) align very closely confirming that the single crystal is representative of the bulk. Elemental microanalysis (CHN) was also carried out and showed good agreement with the theoretical values based on the solved structure for compound **3**. Expected: C 25.19%, H 2.96%, N 2.94%. Found: C 25.31%, H 2.83%, N 2.91%.

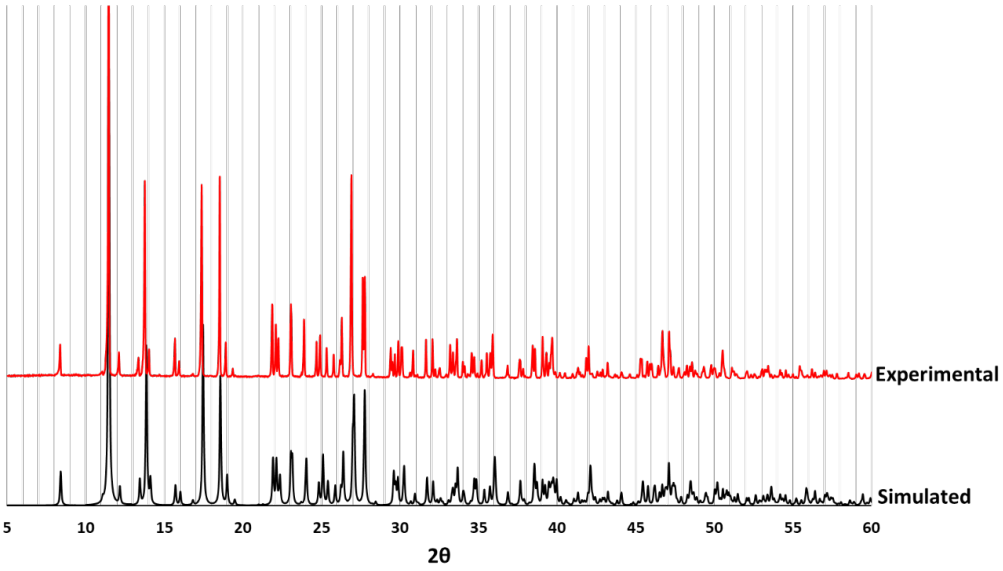


**Figure S9.** Comparison of simulated and experimental PXRD for compound **3**.

Thermogravimetric analysis results are presented in Figure S10.

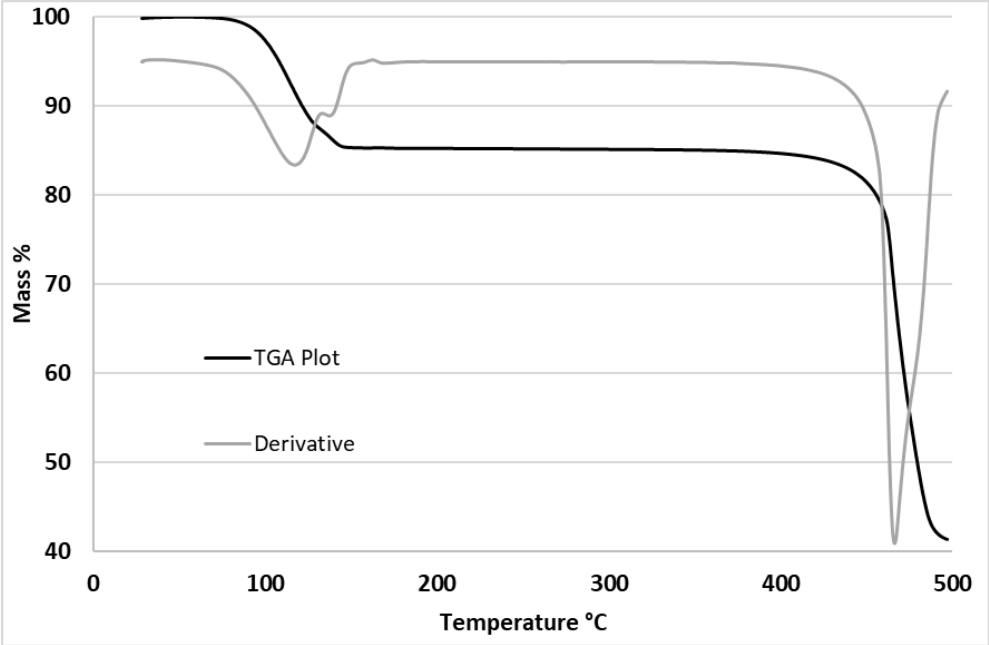


**Figure S10.** Thermogravimetric analysis of compound **3**.

The IR spectrum of compound **3** is shown in Figure S11: (solid, $cm^{-1}$) 3251w, 3184s (br), 1608m, 1572s, 1534m, 1362s, 1318m, 1090w, 813m, 774s, 721s.

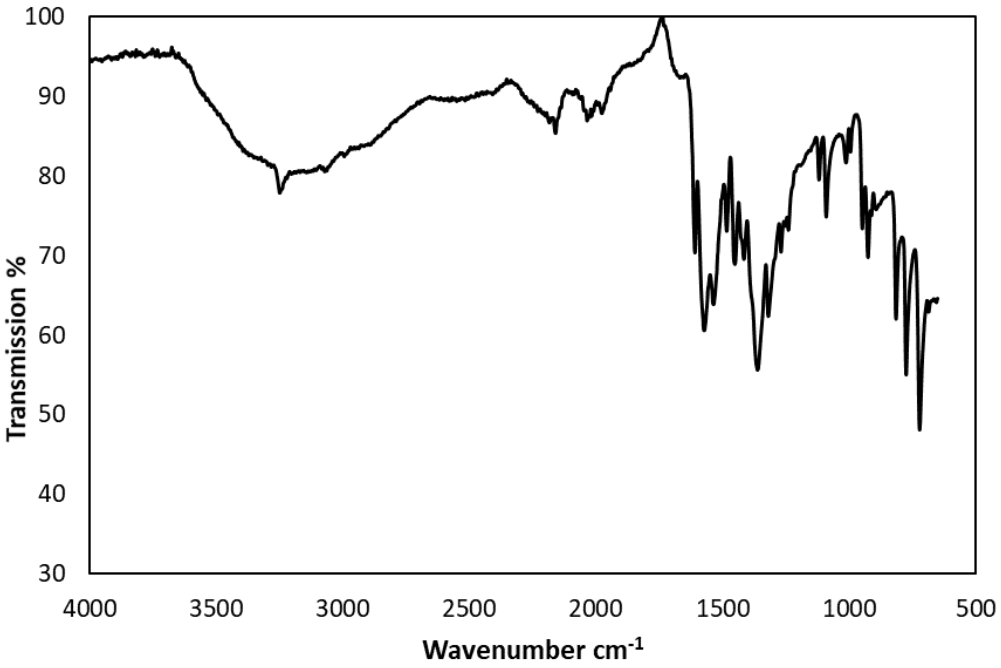


**Figure S11.** Infrared spectrum of compound **3**.

### 2.5 *Synthesis of [$Cd_3(cmai)_2$] (**4**)*

A small sample of compound **3** (*ca.* 40 mg) was heated to 100 °C under reduced pressure using a high vacuum line for a period of 6 hours. During this time, compound **4** was formed and analysis was carried out without further purification. PXRD analysis of compound **4**, presented in Figure S12, shows the bulk material identity is the same as the single crystal data collected for compound **4**. Figure S13 shows PXRD patterns confirming the conversion of **3** to **4** on heating, then re-conversation to **3** on treatment with water.

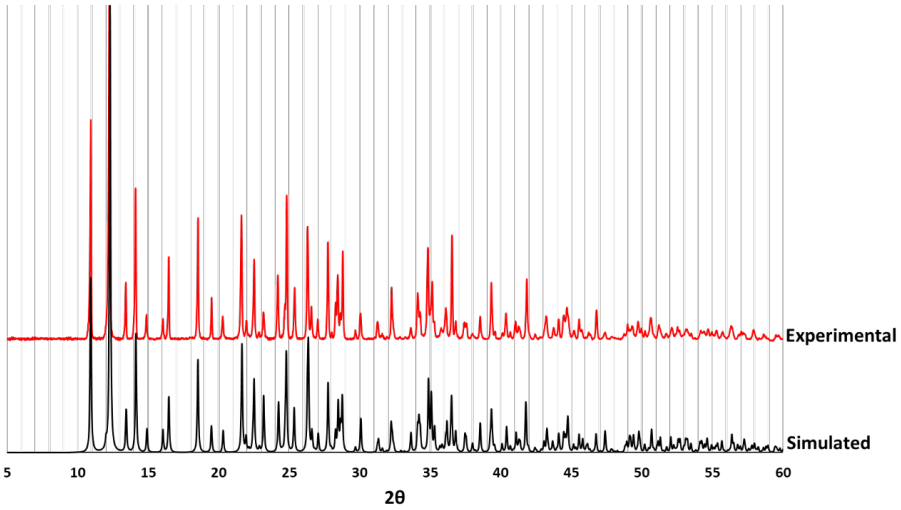


**Figure S12.** Comparison of the simulated and experimental PXRD patterns for compound **4**.

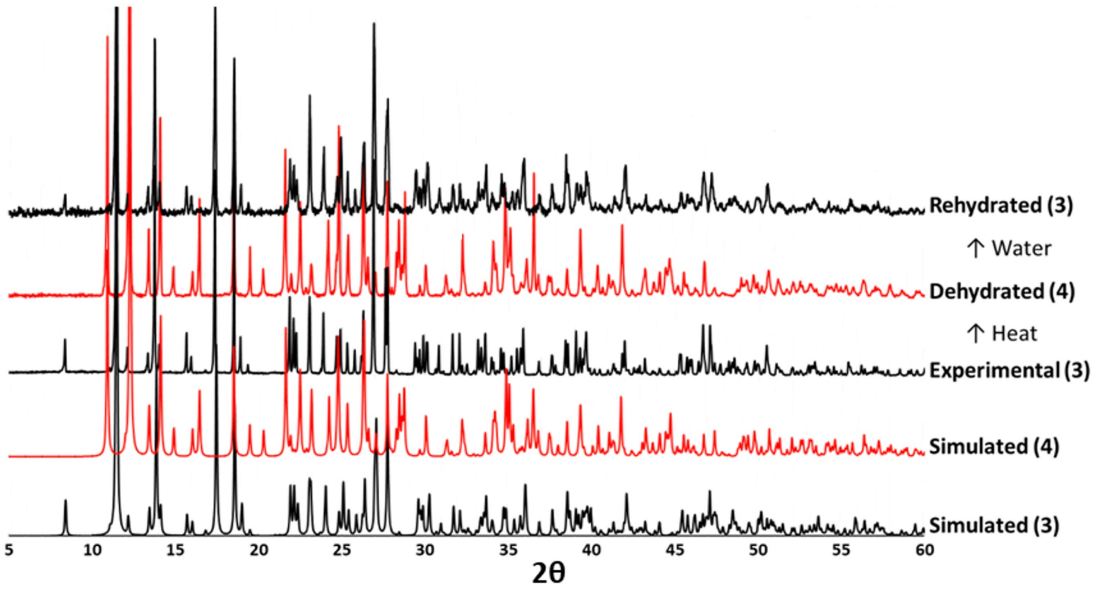


**Figure S13.** PXRD patterns showing the changes occurring on dehydration and rehydration of **3**: from the bottom upwards the traces show the simulated pattern of **3** (from the single crystal structure), the simulated pattern for **4**, the experimental pattern of **3**, the pattern of dehydrated **3** (i.e. **4**) and the pattern collected for rehydrated **4** (i.e. **3**).

The IR spectrum of compound **4** is shown in Figure S14 (solid, $cm^{-1}$) 3320w, 3028w, 1612w (sh), 1572m, 1531m, 1515m, 1490m, 1414s, 1379s, 1083w, 912m, 776s, 728s.

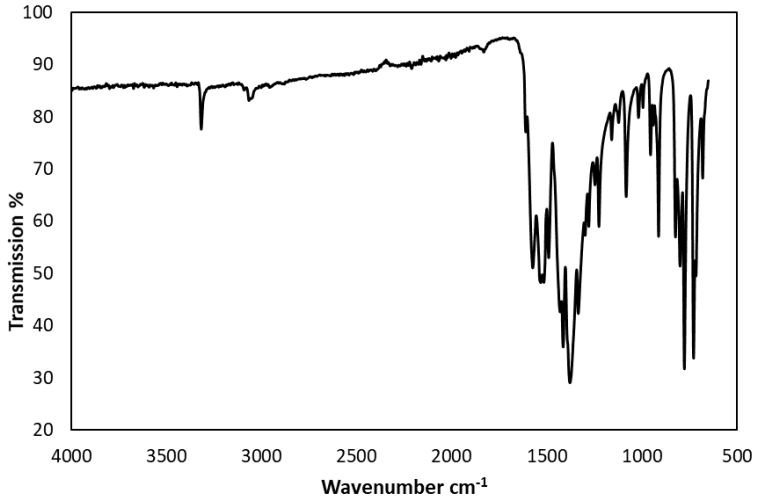


**Figure S14.** Infrared spectrum of compound **4**.

### *2.6 Variable Temperature Powder Diffraction Experiments*

A sample of compound **3** was ground into a fine powder and mounted into a capillary. The capillary was placed into the furnace of a STOE Powder Diffraction System outfitted with a Eurotherm 2416 high temperature device. Scans were collected throughout the experiment using copper radiation in Debye-Scherrer mode and a Multi-MYTHEN detector with a collection time of 10 minutes per trace. During the collection of each pattern the temperature was maintained at a constant value. The temperature profile and collections are described in Table S1.

**Table S1.** The temperature profile and collections for VT-PXRD on compound **3**.

| Time (mins) | Collection /Ramp | Temperature (°C) | | Time (mins) | Collection /Ramp | Temperature (°C) |
|---|---|---|---|---|---|---|
| 0-10 | 1 | 20 | | 75-85 | 7 | 140 |
| 10-12 | Ramp | 40 | | 85-87 | Ramp | 150 |
| 12-22 | 2 | 40 | | 87-92 | Hold | 150 |
| 22-25 | Ramp | 60 | | 92-102 | 8 | 150 |
| 25-35 | 3 | 60 | | 102-107 | Hold | 150 |
| 35-37 | Ramp | 80 | | 107-117 | 9 | 150 |
| 37-48 | 4 | 80 | | 117-122 | Hold | 150 |
| 48-50 | Ramp | 100 | | 122-132 | 10 | 150 |
| 50-60 | 5 | 100 | | 132-138 | Hold | 150 |
| 60-62 | Ramp | 120 | | 138-148 | 11 | 150 |
| 62-73 | 6 | 120 | | 148-167 | Ramp | 20 |
| 73-75 | Ramp | 140 | | 167-177 | 12 | 20 |

### *2.7 Synthesis of $[Cd_6(cmai)_4(H_2O)_{9.75}(DMF)_{2.25}]\cdot 20H_2O\cdot 1.6DMF$ (**5**)*

$H_3$cmai (0.4 mmol, 0.0960 g) was added to 16 mL of DMF and sonicated for 15 mins after which time 16 mL of $H_2O$ was added causing dissolution of the acid. To the solution was added $Cd(NO_3)_2\cdot 4H_2O$ (1.2 mmol, 0.0960 g). The solution remained slightly cloudy and was split between 7 smaller vials to facilitate evaporation and left for 48 hours in a fume hood after which time large colourless block shaped crystals had formed. The samples were combined and the crystals collected via vacuum filtration, washing with deionised water and then stored in fresh deionised water until required. Elemental microanalysis (CHN): Expected: C 25.41%, H 4.57%, N 4.51%. Found: C 26.25%, H 4.24%, N 4.92%. The slightly higher than expected percentages for carbon and nitrogen suggest that the DMF pore content may be, on average, greater than that suggested by the data collected for the selected single crystal.

The simulated and experimental PXRD patterns (Figure S15) correspond closely confirming that the singe crystal structure is representative of the bulk material.

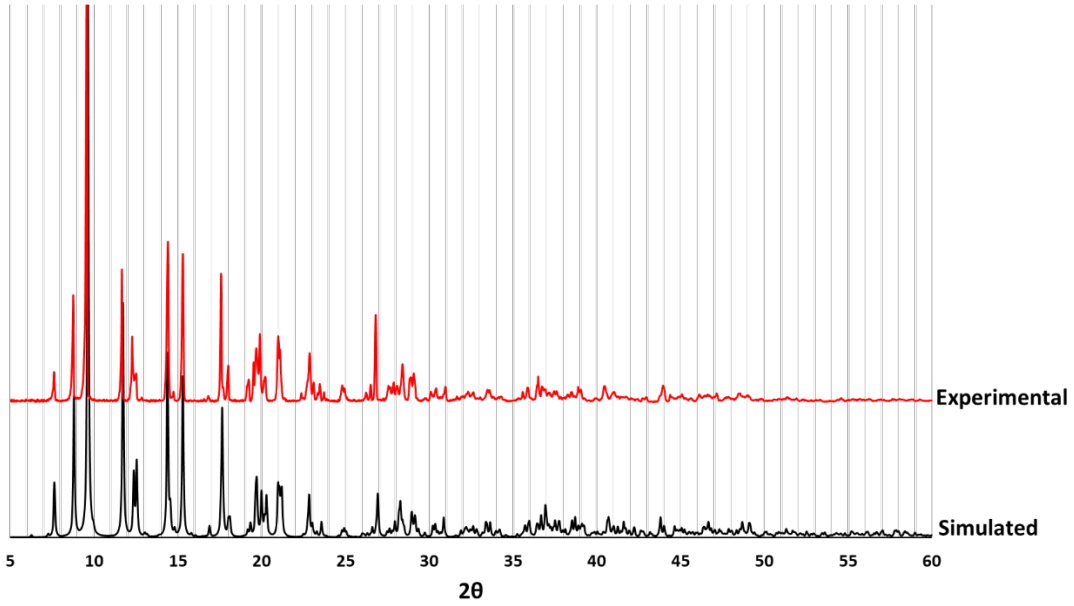


**Figure S15.** Comparison of simulated and experimental PXRD patterns for compound **5**.

Thermogravimetric analysis results are presented in Figure S16.

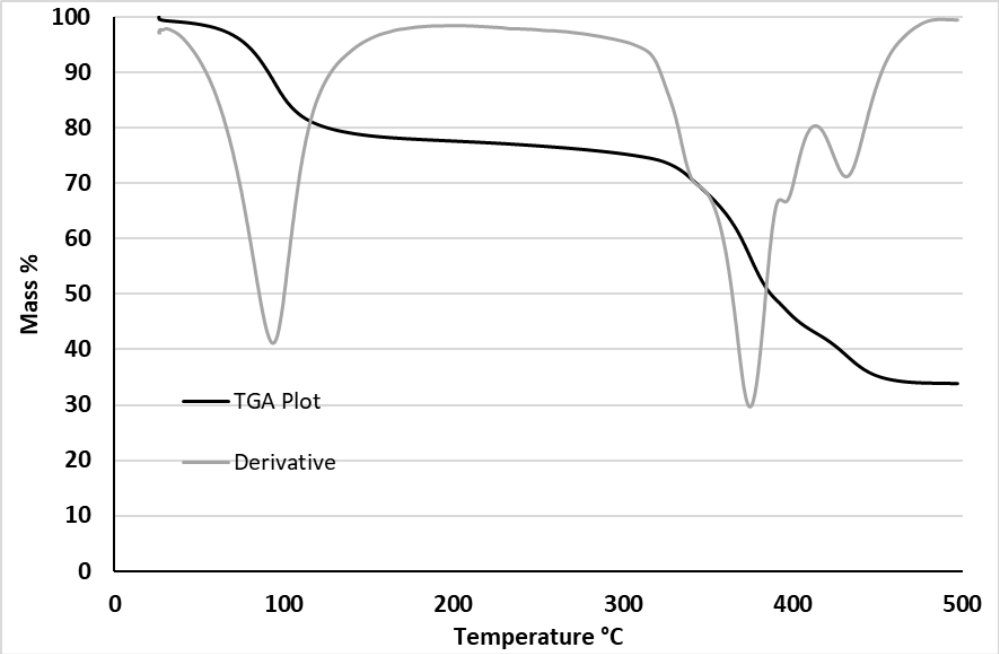


**Figure S16.** Thermogravimetric analysis of compound **5**.

The IR spectrum of compound **5** is shown in Figure S17: (solid, $cm^{-1}$) 3283vs (br), 1648m, 1574s, 1372s, 1305s, 1109w, 919w, 779s, 735s.

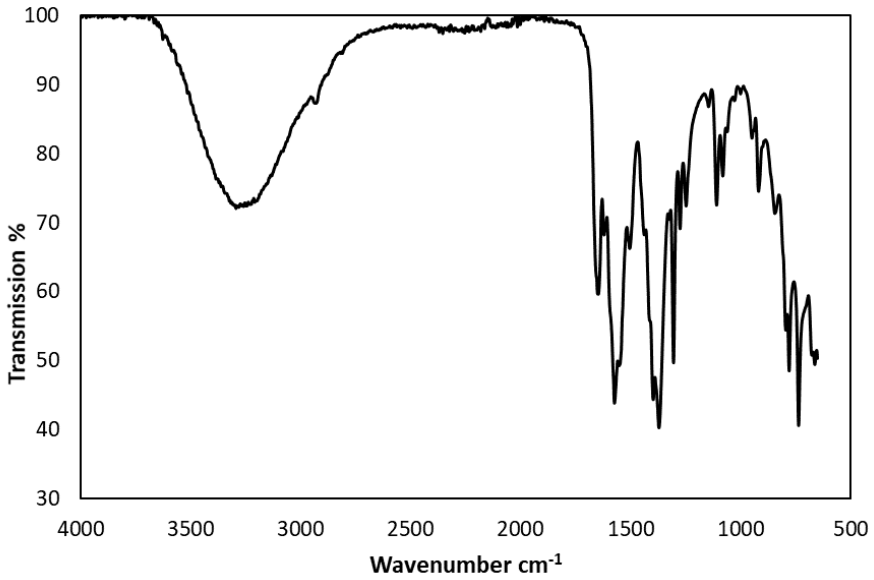


**Figure S17.** Infrared spectrum of compound **5**.

### *2.8 Synthesis of $[Cd_3(cmai)_2(H_2O)_3]\cdot 6H_2O$ (**6**)*

$H_3$cmai (0.1 mmol, 0.0239 g) was placed in a 10 mL microwave vial containing 4 mL of DEF and the mixture was sonicated for 15 minutes. To this was added 4 mL of water, causing the acid to fully dissolve. 4,4'-bypyridine (bipy) (0.1 mmol, 0.0154 g) followed by $Cd(NO_3)_2\cdot 4H_2O$ (0.3 mmol, 0.0925 g) were added and the vial was sealed, then placed in an oven at 120 °C for three days. After cooling to room temperature, the colourless plate crystals were collected by vacuum filtration and washed with deionised water and stored in fresh deionised water until required.

The bulk material of compound **6** was analysed by PXRD and the trace compared to that simulated from the single crystal data. As can be seen in Figure S18 the patterns match very closely confirming the identity of the bulk as compound **6**.

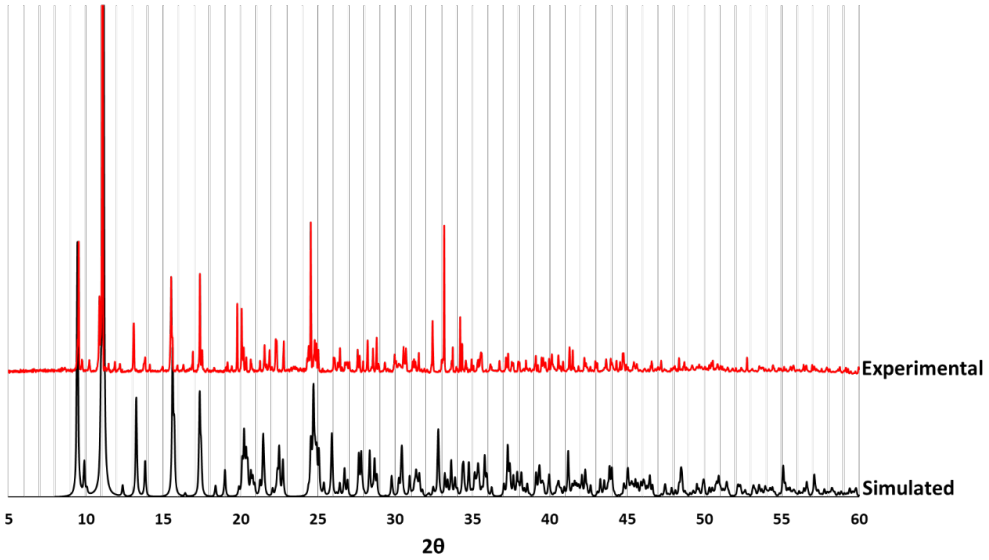


**Figure S18.** A comparison of the experimental PXRD pattern of compound **6** and the pattern simulated from single crystal data.

Thermogravimetric analysis results are presented in Figure S19.

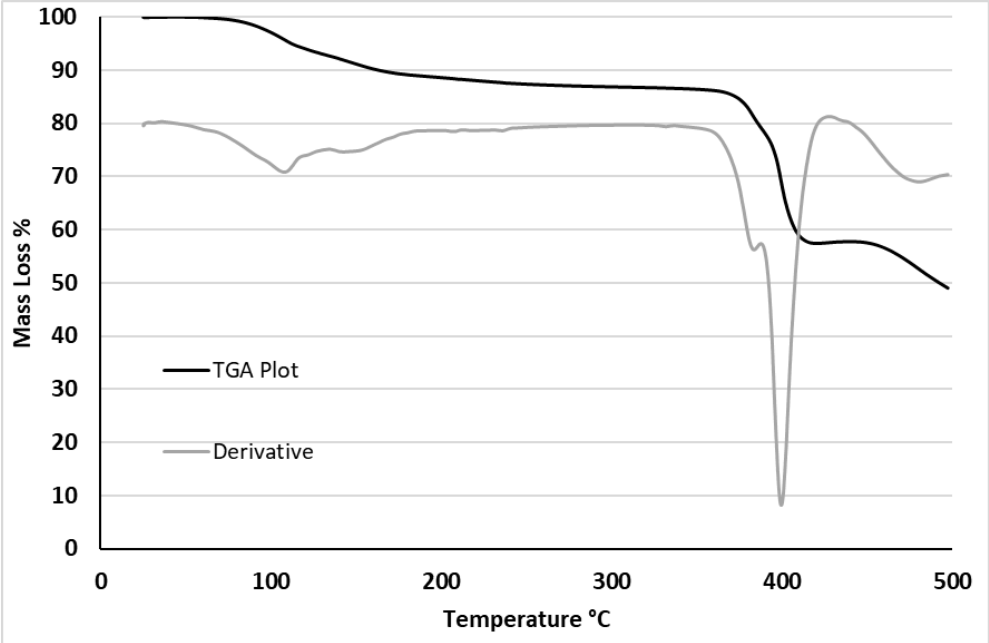


**Figure S19.** Thermogravimetric analysis of compound **6**.

The IR spectrum of compound **6** is shown in Figure S20: (solid, $cm^{-1}$) 3282s (br), 1578m (sh), 1545s, 1425m (sh), 1365s, 1308s, 778s, 727s.

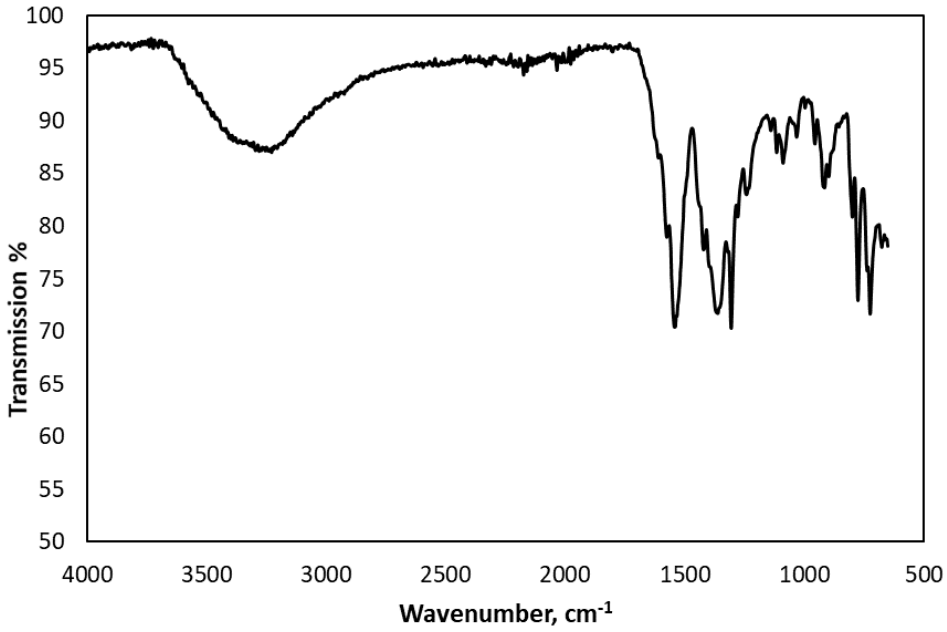


**Figure S20.** Infrared spectrum of compound **6.**

### *2.9 Synthesis of [Zn(Hcmai)($H_2O$)$_2$] (**7**)*

$Zn(NO_3)_2 \cdot 6H_2O$ (0.6 mmol, 0.1785 g) and $H_3$cmai (0.2 mmol, 0.0478 g) were added to a 10 mL microwave vial containing 8mL of $H_2O$ and sonicated for 15 minutes. The vial sealed with a Teflon lined cap was then placed in an oven for 3 days at 90 °C. After cooling to room temperature, the colourless rod-shaped crystals were collected by vacuum filtration and washed with deionised water and stored in fresh deionised water until required. Elemental microanalysis: Expected: C 35.47%, H 3.27%, N 4.14%. Found: C 35.40%, H 3.11%, N 3.96%.

A PXRD pattern was collected for compound **7** and compared to one generated from single crystal data as shown in Figure S21. The two patterns match closely confirming the identity of the bulk as compound **7**.

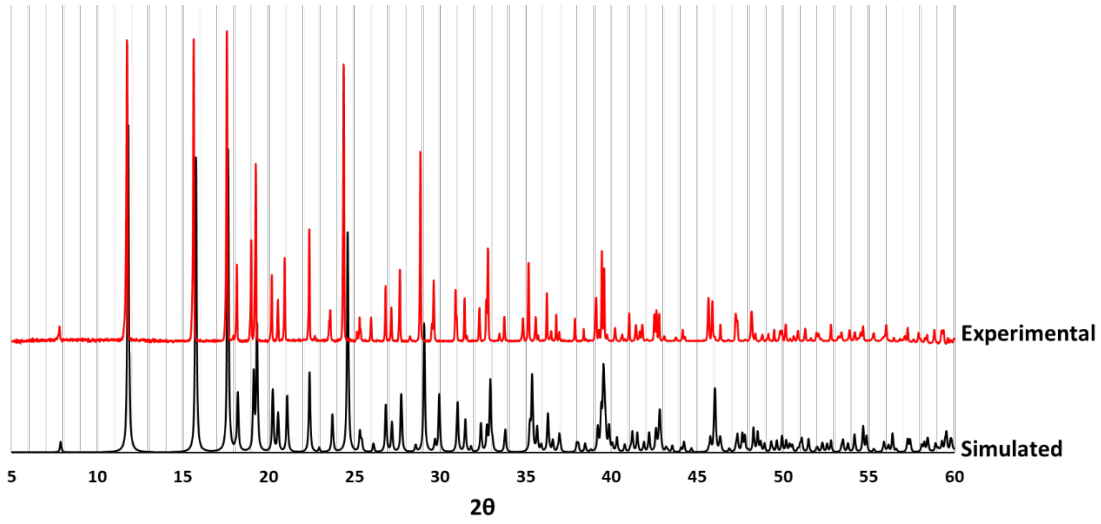


**Figure S21.** The experimental and simulated PXRD patterns for compound **7.**

Thermogravimetric analysis was carried out on compound **7**, the results are presented in Figure S22. The mass loss between 60–195 °C is 4.14%, the expected mass loss for both the coordinated water molecules would be 10.64% suggesting that the majority of the coordinated water remains in the framework until the next mass loss event in the range 225–325 °C of 15.81% The latter represents the remainder of the guest water and some of the organic component of the MOF starting to break down.

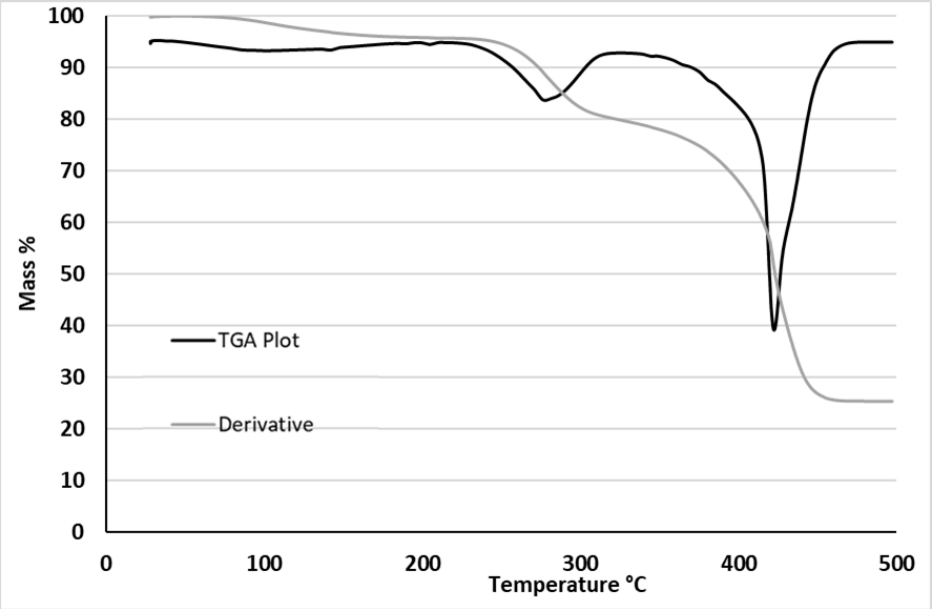


**Figure S22.** Thermogravimetric analysis of compound **7**.

### *2.10 Synthesis of [Cu(Hcmai)($H_2O$)$_{1.2}$] (**8**)*

$Cu(NO_3)_2 \cdot 2.5H_2O$ (0.6 mmol, 0.1396 g) and $H_3$cmai (0.2 mmol, 0.0476 g) were added to 10 mL mixture of EtOH and $H_2O$ in a 1:1 ratio in a Teflon insert for an Parr acid digestion bomb. The mixture was stirred for 15 minutes in the Teflon liner before removing the stirrer bar and sealing the autoclave. The autoclave was heated in an oven at 120 °C for 48 hours. After cooling to room temperature, the clusters of green shard-like crystals were collected by vacuum filtration and washed with deionised water (3 x 3 mL) and fresh ethanol (3 x 3 mL). The crystals were stored in deionised water until required. Elemental microanalysis: Expected: C 37.26%, H 2.94%, N 4.35%. Found: C 37.09%, H 3.12%, N 4.32%.

A PXRD pattern was collected for compound **8** and compared to a pattern simulated from the single crystal data as shown in Figure S23. The two patterns match closely confirming the identity of the bulk as compound **8**.

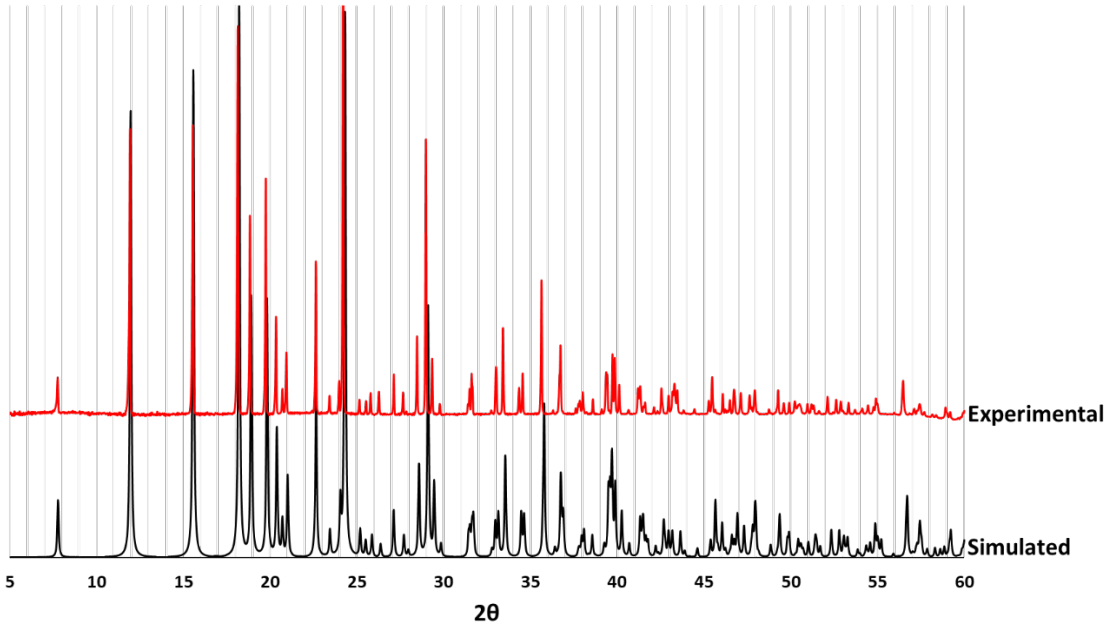


**Figure S23.** The simulated and experimental PXRD patterns for compound **8**.

Thermogravimetric analysis was carried out on compound **8**, the results are presented in Figure S24. The plot shows no mass loss until 200 °C at which point there are three successive events centred on 225 °C, 280 °C, and 320°C which represent water loss from the structure followed by framework decomposition.

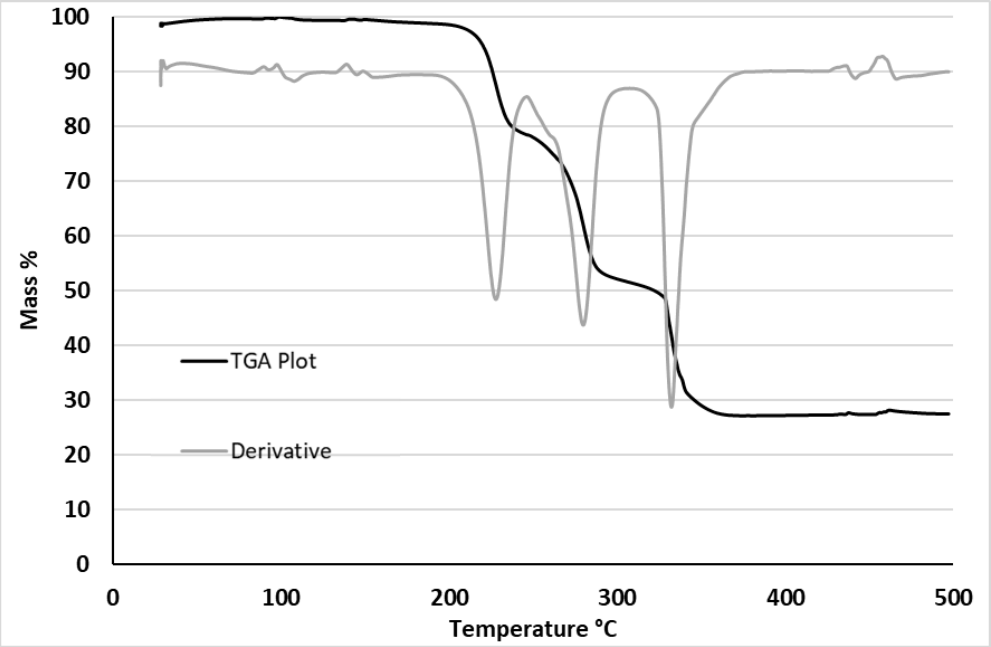


**Figure S24.** Thermogravimetric analysis of compound **8**.

### *2.11 Synthesis of [Co(Hcmai)($H_2O$)$_2$] (**9**)*

$Co(NO_3)_2 \cdot 6H_2O$ (0.5 mmol, 0.1455 g) and $H_3$cmai (0.15 mmol, 0.0359 g) were added to a 10 mL microwave vial containing 8 mL of $H_2O$ and the mixture was sonicated for 15 minutes. The vial sealed with a Teflon lined cap was then placed in an oven for 18 hours at 90 °C. After cooling to room temperature, the pink plate crystals were collected by vacuum filtration and washed with deionised water (3 x 3 mL) and stored in deionised water until required.

Analysis of the bulk material was carried out using PXRD. The collected diffraction pattern was compared to a pattern simulated from the single crystal data and is shown in Figure S25. The two patterns match closely confirming the identity of the bulk as compound **9**.

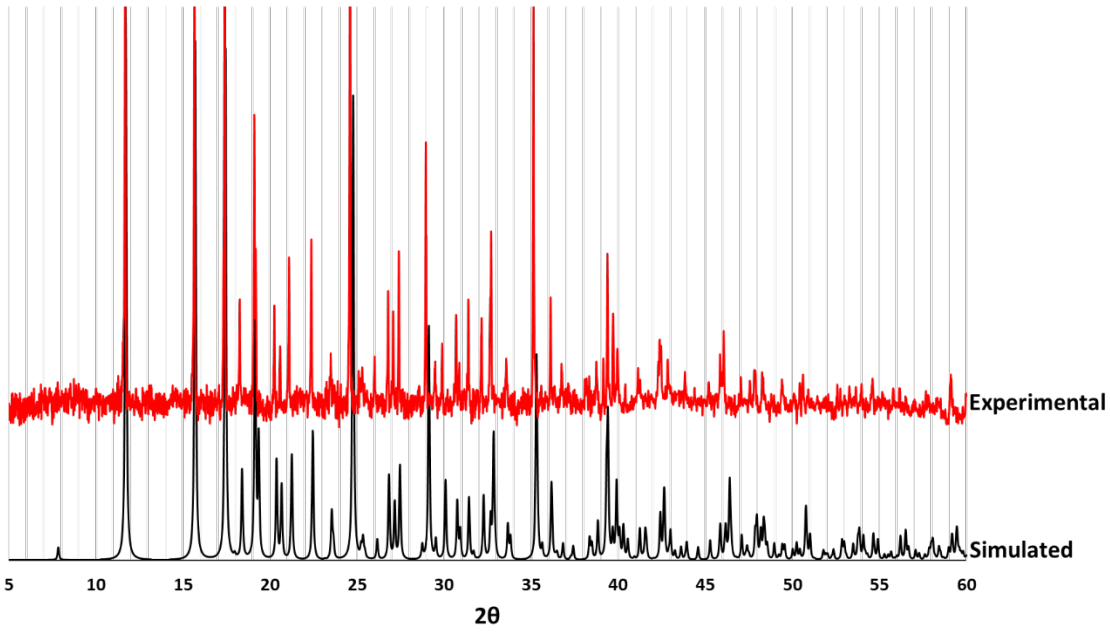


**Figure S25.** The simulated and experimental PXRD traces for compound **9**.

Thermogravimetric analysis results for compound **9** are presented in Figure S26. It can be seen that there is no mass loss observed in the material until 150 °C. There is a slow mass loss between 150–340 °C, equating to 19.1%. This suggests that, as well as the release of the guest water, (which makes up 10.85% of the mass of the material) that some of the organic component also decomposes. After 340 °C there is a sharp increase in the rate of mass loss equating to full decomposition of the remaining linker and residue formation.

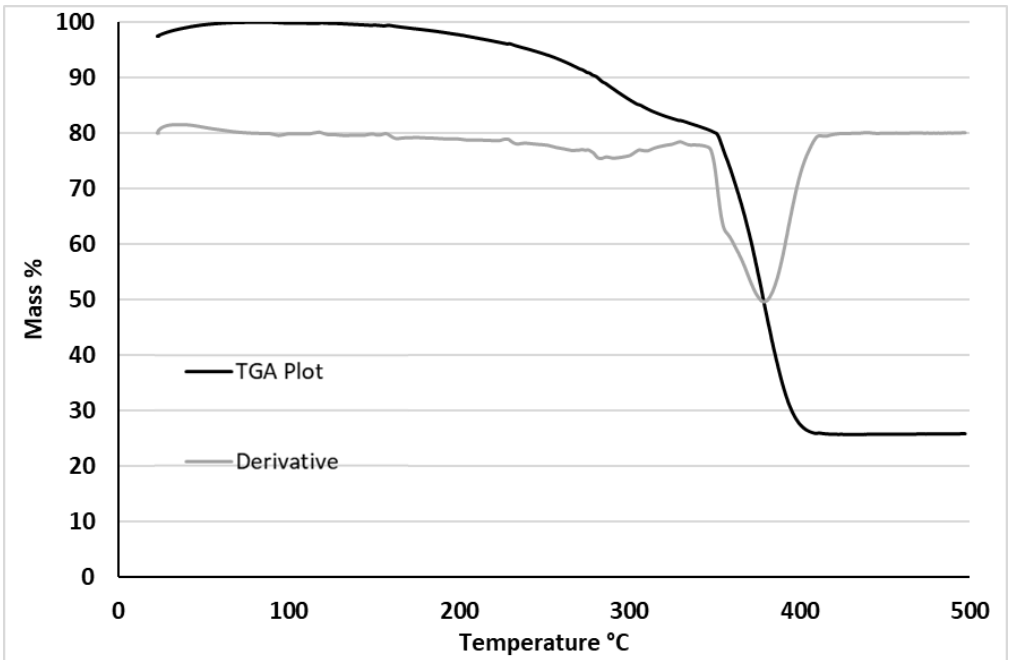


**Figure S26.** Thermogravimetric analysis of compound **9**.

IR spectra for compounds **7**, **8** and **9** are shown in Figure S27.

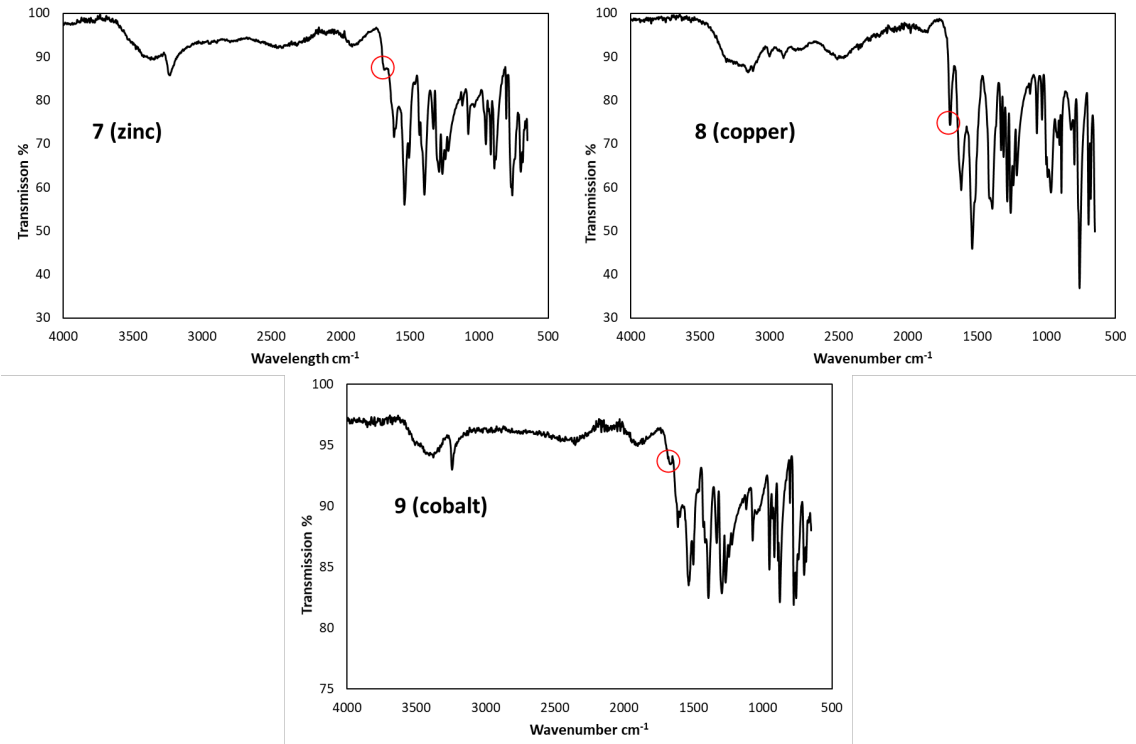


**Figure S27.** Infrared spectra of compounds **7**, **8** and **9**. The highlighted peak represents the carboxlic acid stretch.

### *2.12 Synthesis of $[Zn_2(cmai)(OH)(H_2O)_2]\cdot 3H_2O$ (**10**)*

$Zn(OAc)_2\cdot 2H_2O$ (0.5 mmol, 0.1098 g) and $H_3$cmai were added to a 12 mL of a 50:50 mixture of DEF:water in a 30 mL microwave reaction vial. The vial was sealed, and the mixture sonicated for 15 minutes before being placed in an oven for 72 hours at 120 °C. After cooling to room temperature, the light tan crystals were washed with fresh water (3 x 3 mL) and collected via vacuum filtration at which point they were stored in deionised water until required. Elemental microanalysis: Expected: C 25.34%, H 3.61%, N 2.95%. Found: C 25.21%, H 3.34%, N 2.90%.

A PXRD pattern was collected for compound **10** and compared to a pattern simulated from the single crystal data as shown in Figure S28. The peak positions in the two patterns match well confirming the bulk material as compound **10**.

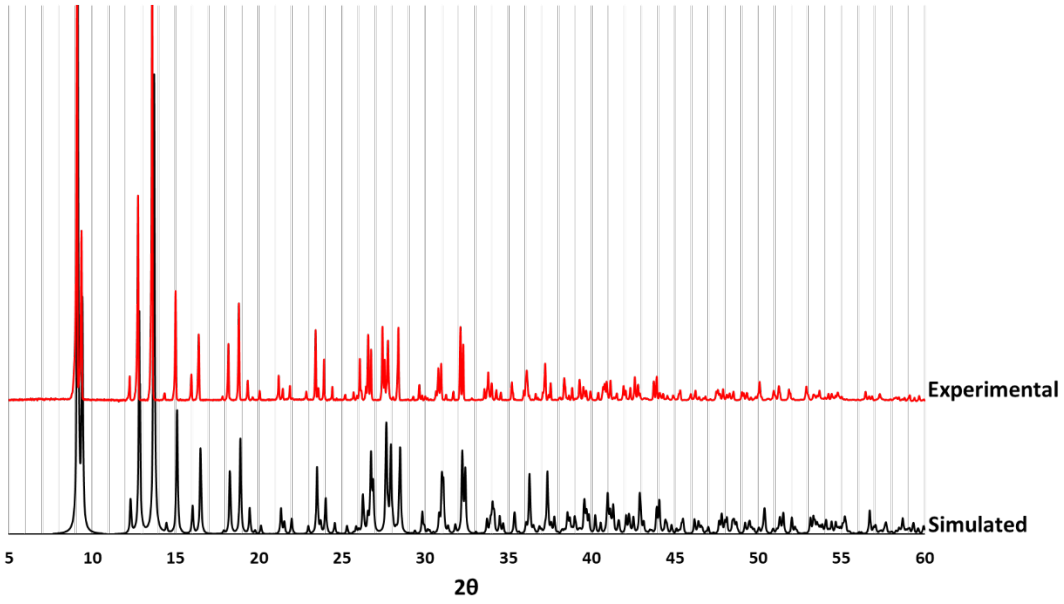


**Figure S28.** The simulated and experimental PXRD traces for compound **10**.

Thermogravimetric analysis results are presented in Figure S29.

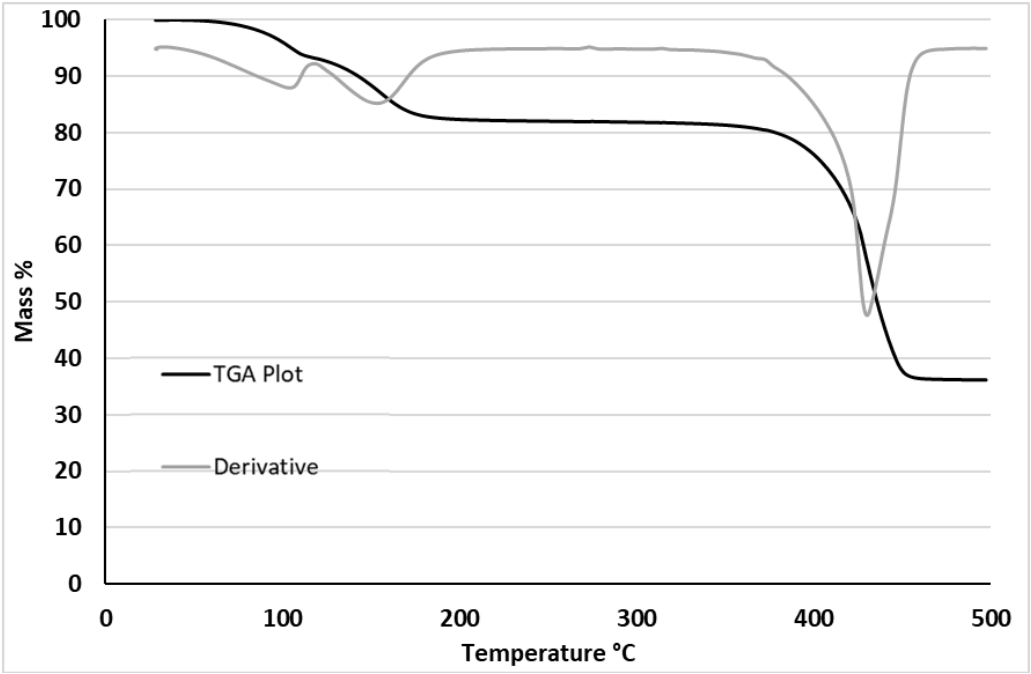


**Figure S29.** Thermogravimetric analysis of compound **10.**

The IR spectrum for compound **10** is presented in Figure S30 (solid, $cm^{-1}$) 3284s (br), 1616m (sh), 1561s, 1407s, 1365s, 1238w, 1090w,1047w, 921w, 780m, 723s.

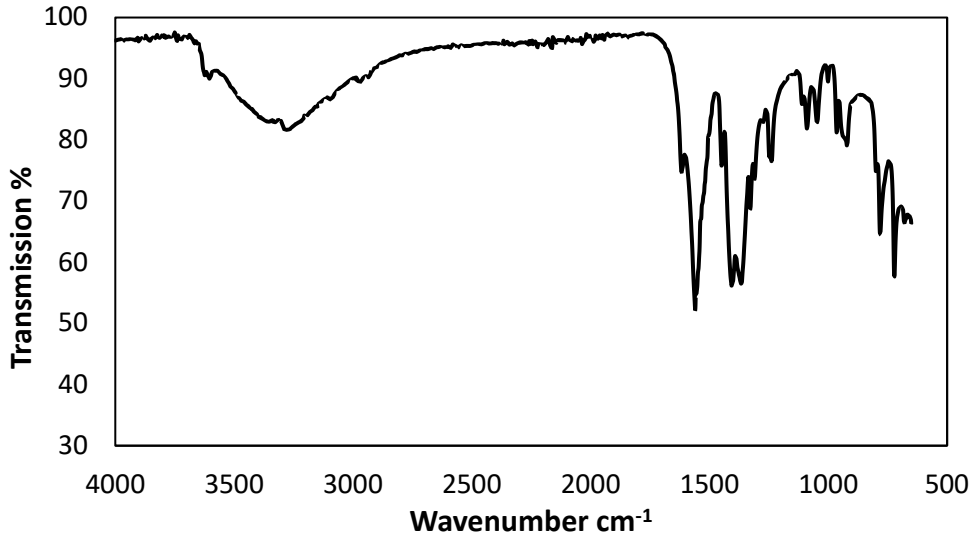


**Figure S30.** Infrared spectrum for compound **10**.

## 3. Crystallography

Data for **1-2**, **8** and **10** were obtained on an Agilent Xcalibur diffractometer and Mo-$K_\alpha$ X-rays (λ = 0.71073 Å), whereas those for **3-7** and **9** were collected using an Agilent SuperNova instrument and a

Cu-$K_\alpha$ source (λ = 1.54184 Å). All experiments were conducted at 150 K with the exception of **5**, for which data were collected at 220 K. Structures were uniformly refined using SHELXL[S1] *via* Olex2.[S2] Crystallographic details for compounds **1-10** are given in Tables S2-4 (page S26) and points of note are detailed below.

The asymmetric unit in **1** comprises two cadmium centres, two Hcmai ligands, two water ligands and one lattice water. The largest residual peak and hole in the difference electron density map are in the region of Cd2 and the ADP for this atom is elongated. Attempts were made to model disorder for Cd2, but these were ultimately abandoned as a similar (obligatory) disorder could not be modelled for the atoms ligated to each disordered component of the metal. Overall, 2-D polymeric sheets dominate the gross structure and these propagate in the *ab* plane. The water hydrogens, along with those bound to N1, N2, O6 and O12, were located and refined at a distance of 0.98 Å from the relevant parent atom. Additional distance restraints (2.75 Å for Cd2···H14a and Cd2···H14b, and 1.5Å for H14a···H14b) were included, to assist convergence. The least reliable hydrogen positions pertain to H14a and H14b. All of the 'located' hydrogens are implicated in hydrogen bonding, which links the coordinatively-bonded sheets, which stack along *c*, to form a 3-D network in the gross structure.

In **2**, the asymmetric unit contains one full-occupancy cadmium centre, one Hcmai ligand and two co-ordinated waters. Oxygen and nitrogen bound hydrogens were readily located and each refined at a distance of 0.98 Å from the relevant parent atom. All O- and N- bound hydrogen atoms are implicated in hydrogen bonding, the result of which is the linking together of the 1-D polymers into the gross structure.

Compound **3** has an asymmetric unit composed of one full cadmium centre, a half cadmium centre which sits on a centre of inversion, one cmai ligand, two co-ordinated water ligands (one to each of the cadmium centres) and two guest water molecules. All water hydrogens and the amine hydrogen were included at readily located positions and each refined at a distance of 0.98 Å from the relevant parent atom. The hydrogens in the water molecule based on O10 were restrained to being a distance of 1.52 Å away from each other to assist convergence, and the $U_{iso}$ values for all water hydrogens were refined freely.

The asymmetric unit in **4** contains one full cadmium centre (Cd1), one half-occupancy cadmium centre (Cd2) and one full cmai moiety. Overall, the structure is a dense 3-D network, consolidated by hydrogen bonding between the amine hydrogen atom in one motif and O1 in a proximate motif. The diffraction pattern was not of premium quality for this sample. The data were integrated initially to take account of twinning, but the level of peak overlap rendered it difficult to de-convolute the data for the components present. Ultimately, the raw data were integrated by increasing the integration mask (1.5 × default mask size) and profile size permitted to alter with incident angle. Essentially, this treated split peaks as arising from a slightly cracked crystal rather than a well-defined twin. The latter approach gave the most satisfactory residuals and $R_{int}$. A side-by-side comparison of the outputs from

both data treatments showed that the optimal one (chosen here) did not negatively impact on the ESDs associated with the bond/angle metrics. The completeness of the data set is less than ideal, but the structure is unambiguous.

Compound **5** crystallises in a monoclinic space group $P2_1$, and was something of a challenge to solve and refine. Inherent diffraction weaknesses, most likely related to pseudosymmetry involving the cadmium centres and their dominance in the reflection intensities, automatically predicted solution in space group *C*2. The higher symmetry carried gave a consequent reduction in the size of the asymmetric unit (by 50%) but there was also concomitant invisibility of the guest solvent and inability to resolve the ligated DMF. Ultimately, examination of calculated diffraction nets, from the raw data frames led to identification of the correct space group symmetry. The asymmetric unit contains six cadmium centres, four cmai linkers, nine full water ligands, two partial water ligands, one full DMF ligand and two partial DMF ligands. There is also a substantial amount of guest solvent, of which only 0.6 DMF molecules were resolved fully. Additional electron density that equates to a mixture of water and DMF (18:0.9 molecules, respectively) was addressed using the solvent mask algorithm available in Olex2. The gross structure builds up into a three-dimensional lattice with convoluted cavities and channels in which the guest solvent resides.

Compound **6** has an asymmetric unit that contains three cadmium centres, two cmai linkers, three water ligands and a total of six guest water molecules. The hydrogen atoms on the water molecules and amine of cmai were included at calculated positions and were corroborated by their implication in an extensive hydrogen-bonding network. The gross structure affords a 3-D MOF with solvent water located in the pores. The refinement took account of racemic twinning of the sample.

The asymmetric unit in **7** contains one full zinc centre, one Hcmai ligand and two co-ordinated water ligands. H1, attached to N1, was readily found and refined subject to being located at a distance of 0.98 Å from its parent. All other hydrogens (including the carboxylic acid hydrogen, H6) were included at calculated positions. The $U_{iso}$ values for H1 and H6 were refined freely.

The asymmetric unit of **8** comprises one full copper centre, one cmai ligand, one full-occupancy co-ordinated water ligand, and a water ligand with 20% occupancy, based on O8. The hydrogen atoms attached to O6, N1 and O7 were located, and subsequently refined at a distance of 0.98 Å from their relevant parent atoms. The hydrogens attached to O8 were included at calculated positions, and the only testament as to their positional credibility lies in the fact that they appear to be implicated in hydrogen bonding. The raw data for this analysis were integrated to take account of crystal twinning, by virtue of a 180$^o$ rotation about the 1, 0, 0 direct axis.

One cobalt centre, one Hcmai ligand, and two water ligands constitute the asymmetric unit in **9**. The water hydrogens, along with those bound to N1 and O6, were located and refined at a distance of 0.98 Å from the relevant parent atom. Additional distance restraints (2.55 Å for Co1···H7a, and 1.5Å

for H7a···H7b) were included, to assist convergence. All of these latter hydrogens are implicated in the formation of a dense hydrogen-bonded network in the lattice.

The asymmetric unit in **10** contains two zinc centres, one cmai ligand, one hydroxide ion, two coordinated water ligands (one to each of the zinc centres) and three guest water molecules. Only one of the latter (based on O10) is ordered; those based on O11 and O12 have been modelled, with ADP restraints, to take account of disorder over five regions in a 25:65:20:80:10 ratio. This disorder is not altogether unsurprising as, in the gross structure (2-D coordinatively bonded sheets, interlinked by hydrogen bonding) the fragment waters reside in channels along the 1,0,1 direction. Hydrogen atoms were not included for the disordered waters, but in the ordered portion of the structure, oxygen and nitrogen bound hydrogens were located and refined at a distance of 0.98 Å from the relevant parent atom. The residual electron density maximum is located at 1.64 Å from O2, and is chemically insignificant. The spurious nature of this peak may arise from the fact that there is evidence of some twinning (136° about the –0.2, 0.95, 0.21 vector) in the raw data frames. However, the level of twinning ( < 5%) did not merit retention in the final refinement.

Crystallographic data for all compounds have been deposited with the Cambridge Crystallographic Data Centre as supplementary publications CCDC 2097428-2097437 for **1-10**, respectively. Copies of these data can be obtained free of charge on application to CCDC, 12 Union Road, Cambridge CB2 1EZ, UK [fax: (+44) 1223 336033, e-mail: deposit@ccdc.cam.ac.uk.]

**Table S2.** Crystal data and structural refinement for compounds **1-3.**

| Compound | **1** | **2** | **3** |
|---|---|---|---|
| Empirical formula | $C_{20}H_{20}Cd_2N_2O_{15}$ | $C_{10}H_{11}CdNO_8$ | $C_{20}H_{28}Cd_3N_2O_{20}$ |
| Formula weight | 753.18 | 385.60 | 953.64 |
| Crystal system | monoclinic | triclinic | triclinic |
| Space group | *I*2/*a* | *P*-1 | *P*-1 |
| *a*/ Å | 13.7701(4) | 7.2467(6) | 7.7777(2) |
| *b*/ Å | 11.5100(3) | 8.5509(7) | 8.9715(4) |
| *c*/ Å | 29.1745(7) | 10.9978(6) | 11.4851(4) |
| *α*/ ° | 90 | 101.892(6) | 67.353(4) |
| *β*/ ° | 90.088(2) | 95.728(5) | 75.848(3) |
| *γ*/ ° | 90 | 114.776(8) | 70.505(3) |
| *U*/ Å$^3$ | 4624.0(2) | 592.04(8) | 690.98(5) |
| *Z* | 8 | 2 | 1 |
| $\rho_{calc}$/ g cm$^{-3}$ | 2.164 | 2.163 | 2.292 |
| $\mu$/ mm$^{-1}$ | 1.925 | 1.886 | 19.211 |
| *F*(000) | 2960.0 | 380.0 | 466.0 |
| Crystal size/ mm$^3$ | 0.291 × 0.231 × 0.063 | 0.344 × 0.24 × 0.083 | 0.038 × 0.028 × 0.025 |
| 2$\theta$ range for data collection/° | 7.034 to 60.686 | 6.696 to 60.678 | 8.418 to 146.698 |
| Index ranges | −18 ≤ h ≤ 15,<br>−16 ≤ k ≤ 13,<br>−41 ≤ l ≤ 39 | −10 ≤ h ≤ 9,<br>−8 ≤ k ≤ 12,<br>−15 ≤ l ≤ 15 | −9 ≤ h ≤ 9,<br>−11 ≤ k ≤ 11,<br>−12 ≤ l ≤ 14 |
| Reflections collected | 21531 | 5470 | 13561 |
| Independent reflections, $R_{int}$ | 6180, 0.0246 | 2988, 0.0323 | 2755, 0.0386 |
| Data/restraints/parameters | 6180/19/390 | 2988/6/205 | 2755/12/241 |
| Goodness–of–fit on F$^2$ | 1.074 | 1.069 | 1.026 |
| Final *R*1, *wR*2 [*I*>=2σ(*I*)] | 0.0321, 0.0638 | 0.0335, 0.0636 | 0.0199, 0.0489 |
| Final *R*1, *wR*2 [all data] | 0.0373, 0.0659 | 0.0376, 0.0668 | 0.0216, 0.0496 |
| Largest diff. peak/hole/ e Å$^{-3}$ | 1.66/−3.60 | 0.95/−0.71 | 0.51/−0.62 |
| Flack parameter | – | – | – |

**Table S3.** Crystal data and structural refinement for compounds **4-6**

| Compound | **4** | **5** | **6** |
|---|---|---|---|
| Empirical formula | $C_{20}H_{12}Cd_3N_2O_{12}$ | $C_{51.25}H_{105.75}Cd_6N_{7.75}O_{55.5}$ | $C_{20}H_{30}Cd_3N_2O_{21}$ |
| Formula weight | 809.52 | 2393.08 | 971.66 |
| Crystal system | triclinic | monoclinic | monoclinic |
| Space group | *P*-1 | $P2_1$ | $P2_1$ |
| *a*/ Å | 8.0862(15) | 14.1081(1) | 9.0126(1) |
| *b*/ Å | 8.1863(13) | 14.3068(2) | 18.6624(1) |
| *c*/ Å | 8.4893(11) | 23.1617(3) | 9.1644(1) |
| *α*/ ° | 72.651(13) | 90 | 90 |
| *β*/ ° | 81.681(13) | 90.945(1) | 103.467(1) |
| *γ*/ ° | 65.767(17) | 90 | 90 |
| *U*/ Å$^3$ | 488.97(15) | 4674.36(10) | 1499.04(3) |
| *Z* | 1 | 2 | 2 |
| $\rho_{calc}$/ g cm$^{-3}$ | 2.749 | 1.700 | 2.153 |
| $\mu$/ mm$^{-1}$ | 26.648 | 11.633 | 17.751 |
| *F*(000) | 386.0 | 2399.0 | 952.0 |
| Crystal size/ mm$^3$ | 0.064 × 0.033 × 0.015 | 0.11 × 0.085 × 0.031 | 0.218 × 0.104 × 0.036 |
| 2θ range for data collection/° | 12.006 to 136.352 | 6.266 to 146.148 | 9.478 to 146.104 |
| Index ranges | −8 ≤ h ≤ 9,<br>−9 ≤ k ≤ 9,<br>−10 ≤ l ≤ 10 | −16 ≤ h ≤ 17,<br>−17 ≤ k ≤ 15,<br>−28 ≤ l ≤ 28 | −11 ≤ h ≤ 7,<br>−23 ≤ k ≤ 20,<br>−11 ≤ l ≤ 11 |
| Reflections collected | 2549 | 66896 | 10096 |
| Independent reflections, $R_{int}$ | 1632, 0.0286 | 17026, 0.0446 | 5352, 0.0376 |
| Data/restraints/parameters | 1632/1/173 | 17026/219/1020 | 5352/3/449 |
| Goodness–of–fit on F$^2$ | 1.045 | 1.013 | 1.072 |
| Final *R*1, *wR*2 [*I*>=2σ(*I*)] | 0.0488, 0.1187 | 0.0626, 0.1711 | 0.0418, 0.1045 |
| Final *R*1, *wR*2 [all data] | 0.0614, 0.1273 | 0.0648, 0.1735 | 0.0418, 0.1045 |
| Largest diff. peak/hole/ e Å$^{-3}$ | 1.88/−1.31 | 3.79/−1.51 | 2.10/−1.13 |
| Flack parameter | – | 0.419(13) | 0.426(12) |

**Table S4.** Crystal data and structural refinement for compounds **7-10.**

| Compound | **7** | **8** | **9** | **10** |
|---|---|---|---|---|
| Empirical formula | $C_{10}H_{11}NO_8Zn$ | $C_{10}H_{9.4}CuNO_{7.2}$ | $C_{10}H_{11}CoNO_8$ | $C_{10}H_{17}NO_{12}Zn_2$ |
| Formula weight | 338.57 | 322.32 | 332.13 | 473.98 |
| Crystal system | monoclinic | monoclinic | monoclinic | monoclinic |
| Space group | $P2_1$ | $P2_1$ | $P2_1$ | $P2_1/n$ |
| $a$/ Å | 4.8959(1) | 4.9056(5) | 4.8412(2) | 7.4213(3) |
| $b$/ Å | 10.0630(3) | 9.7392(10) | 10.1675(4) | 19.3205(6) |
| $c$/ Å | 11.3009(4) | 11.4649(14) | 11.3320(4) | 10.8081(4) |
| $\alpha$/ ° | 90 | 90 | 90 | 90 |
| $\beta$/ ° | 95.584(3) | 97.117(10) | 95.158(4) | 96.871(3) |
| $\gamma$/ ° | 90 | 90 | 90 | 90 |
| $U$/ Å$^3$ | 554.12(3) | 543.53(10) | 555.54(4) | 1538.57(10) |
| $Z$ | 2 | 2 | 2 | 4 |
| $\rho_{calc}$/ g cm$^{-3}$ | 2.029 | 1.969 | 1.986 | 2.046 |
| $\mu$/ mm$^{-1}$ | 3.538 | 2.044 | 12.568 | 3.186 |
| $F$(000) | 344.0 | 326.0 | 338.0 | 960.0 |
| Crystal size/ mm$^3$ | 0.141 × 0.041 × 0.023 | 0.316 × 0.089 × 0.019 | 0.183 × 0.046 × 0.033 | 0.277 × 0.239 × 0.105 |
| 2$\theta$ range for data collection/° | 7.86 to 146.822 | 7.164 to 55.04 | 7.834 to 146.51 | 6.664 to 54.958 |
| Index ranges | −6 ≤ h ≤ 6, −10 ≤ k ≤ 12, −14 ≤ l ≤ 13 | −3 ≤ h ≤ 6, −12 ≤ k ≤ 12, −14 ≤ l ≤ 14 | −5 ≤ h ≤ 6, −12 ≤ k ≤ 12, −13 ≤ l ≤ 14 | −9 ≤ h ≤ 9, −24 ≤ k ≤ 25, −14 ≤ l ≤ 14 |
| Reflections collected | 4616 | 2564 | 2451 | 12808 |
| Independent reflections, $R_{int}$ | 1628, 0.0321 | 2564, 0.0541 | 1637, 0.0292 | 3507, 0.0393 |
| Data/restraints/parameters | 1628/2/189 | 2564/5/198 | 1637/10/204 | 3507/40/278 |
| Goodness–of–fit on F$^2$ | 1.068 | 0.953 | 1.044 | 1.081 |
| Final $R$1, $wR$2 [$I$>=2σ($I$)] | 0.0308, 0.0803 | 0.0481, 0.0958 | 0.0461, 0.1224 | 0.0323, 0.0774 |
| Final $R$1, $wR$2 [all data] | 0.0314, 0.0810 | 0.0611, 0.0989 | 0.0472, 0.1241 | 0.0391, 0.0808 |
| Largest diff. peak/hole/ e Å$^{-3}$ | 0.66/−0.49 | 0.56/−1.00 | 0.69/−0.61 | 1.60/−0.49 |
| Flack parameter | −0.09(3) | −0.01(3) | −0.001(6) | – |

The asymmetric units for compounds **1-10** are shown in Figures S31-S40 respectively.

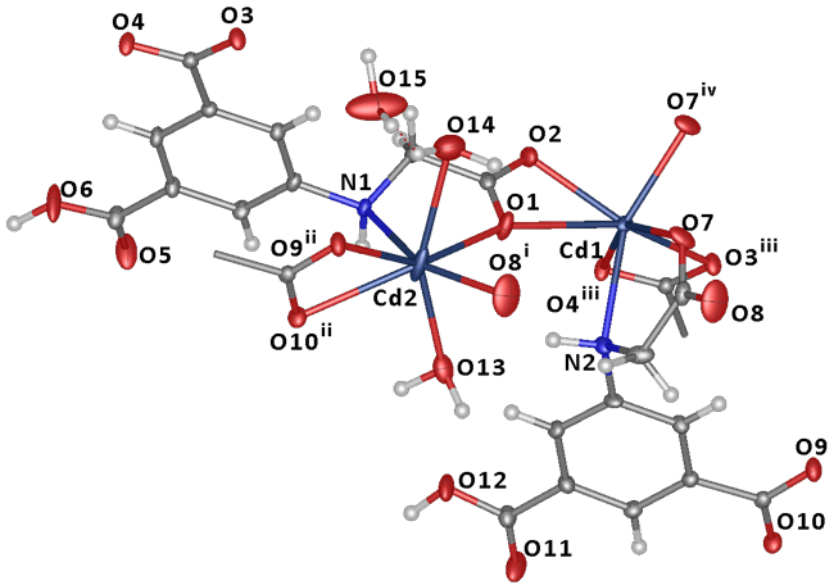


**Figure S31.** The asymmetric unit and cadmium coordination spheres in compound **1**. Atoms with labels containing superscripts are related to those in the asymmetric unit by the following symmetry operations: i, 1 – *x*; 1 –*y*, 1 – *z*; ii, + *x*, – 1 + *y*, + *z*; iii, + *x*, 1 + *y*, + *z*; iv, 3/2 – *x*, + *y*, 1 – *z*. (Atomic displacement parameters (ADPs) are plotted at 50%).

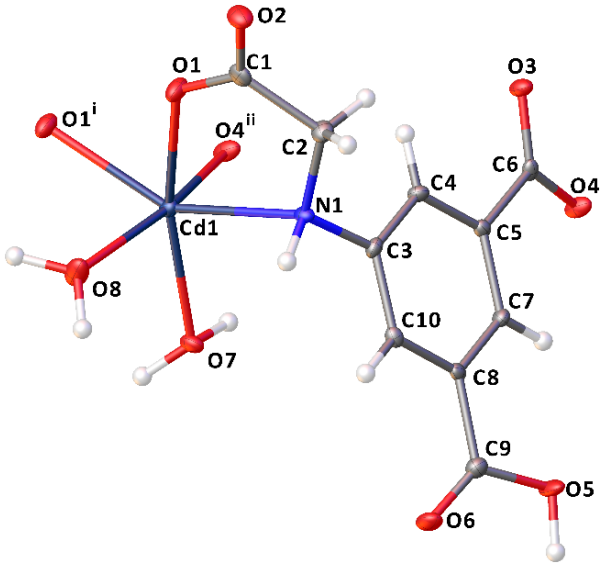


**Figure S32.** The asymmetric unit and cadmium coordination sphere in compound **2.** (i, 2 – *x*, 1 – *y*, – *z*; ii, 2 – *x*, 1 – *y*, 1 – *z*.) (ADPs plotted at 50%).

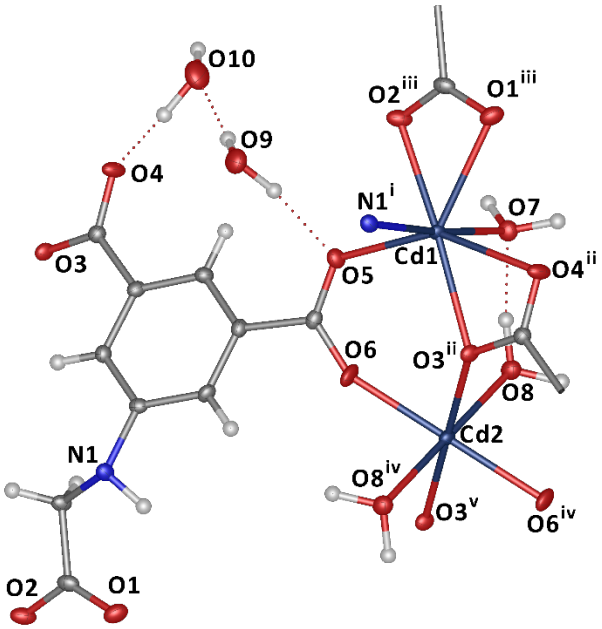


**Figure S33.** The asymmetric unit and coordination sphere of the cadmium centres in compound **3**. (i, 1 – *x*, – *y*, 2 – *z*; ii, 1 + *x*, – 1 + *y*, + *z*; iii, 1 + *x*, + *y*, – 1 + *z*; iv, – *x*, – *y*, 2 – *z*; v, 1 – *x*, – 1 – *y*, 2 – *z*) (ADPs represented at 50% probability).

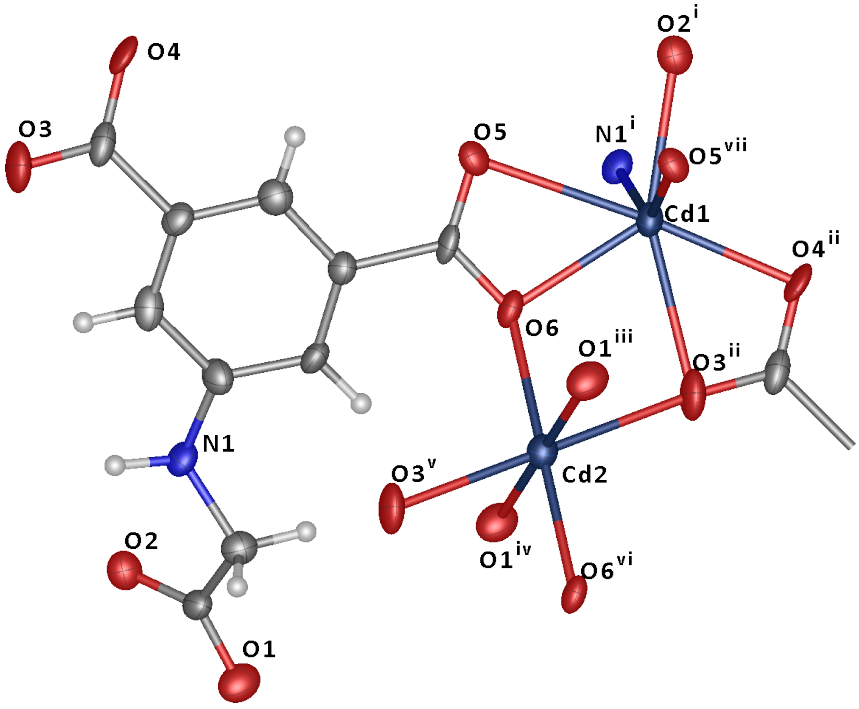


**Figure S34.** The asymmetric unit of compound **4** with coordination spheres of Cd1 and Cd2. (i, 1 – *x*, 1 – *y*, – *z*; ii, + *x*, 1 + *y*, – 1 + *z*; iii, – 1 + *x*, 1 + *y*, + *z*; iv, 2 – *x*, 1 – *y*, – *z*; v, 1 – *x*, 1 – *y*, 1 – *z*; vi, 1 – *x*, 2 – *y*, – *z*; vii, – *x*, 2 – *y*, – *z*) (ADPs represented at 50% probability).

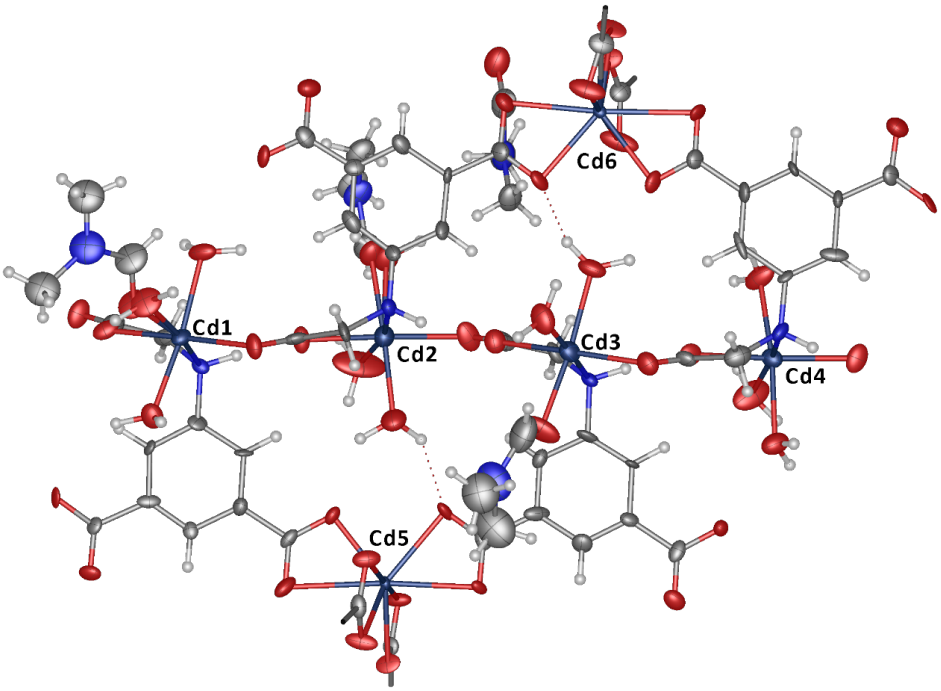


**Figure S35.** The asymmetric unit of compound **5**, along with the coordination sphere of the cadmium centres. (ADPs at 50% probability).

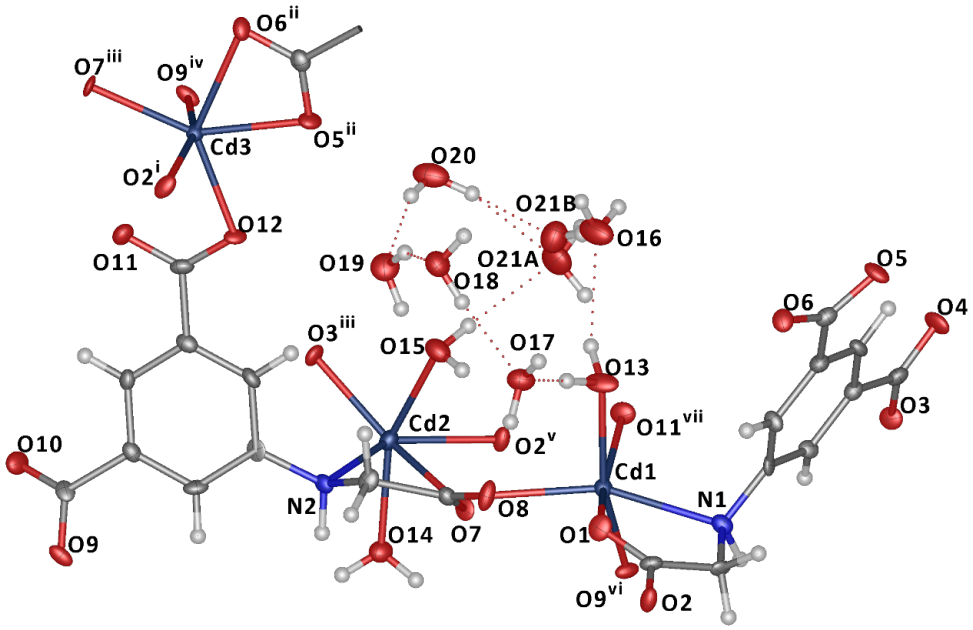


**Figure S36.** The asymmetric unit of compound **6** along with the coordination spheres of the cadmium centres. (i, 1 – *x*, 1/2 + *y*, 1 – *z*; ii, – *x*, 1/2 + *y*, 1 – *z*; iii, 1 – *x*, 1/2 + *y*, 2 – *z*; iv, – 1 + *x*, + *y*, + *z*; v, + *x*, + *y*, 1 + *z*; vi, 2 – *x*, – 1/2 + *y*, 2 – *z*; 1 – *x*, – 1/2 + *y*, 2 – *z*) (ADPs shown at 50% probability).

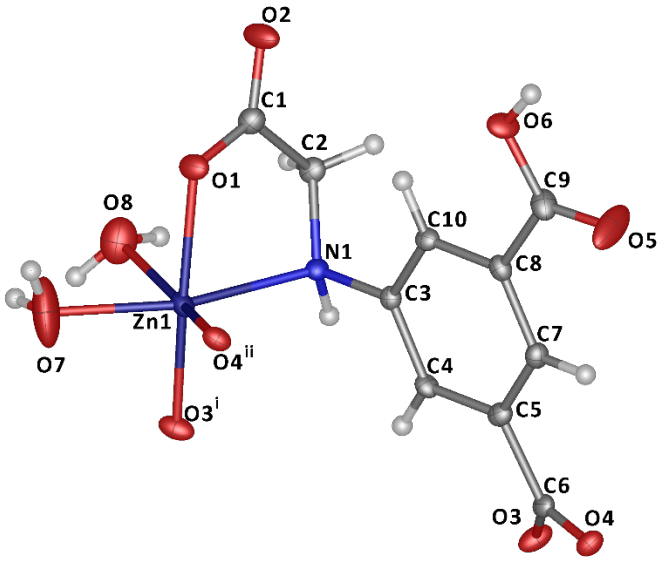


**Figure S37.** The asymmetric unit and coordination sphere in Zn1 of compound **7**. (i, 2 – *x*, – 1/2 + *y*, 2 – *z*; ii, 1 – *x*, – 1/2 + *y*, 2 – *z*.)

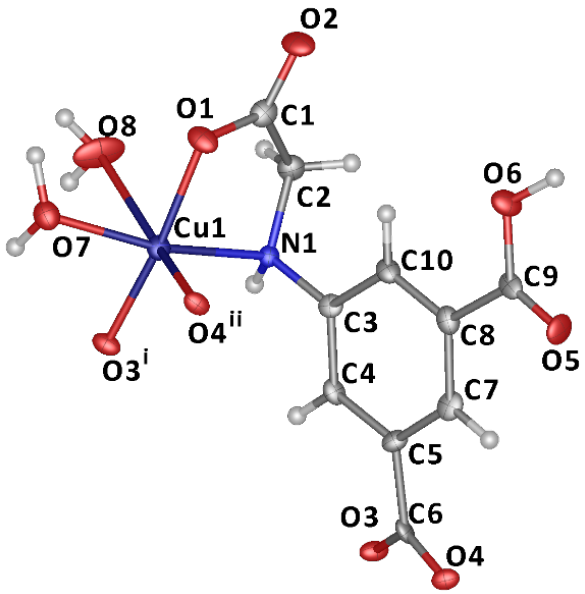


**Figure S38.** The asymmetric unit of compound **8** and coordination sphere of Cu1. (i, 2 – *x*, – 1/2 + *y*, 1 – *z*; ii, 1 – *x*, – 1/2 + *y*, 1 – *z*.)

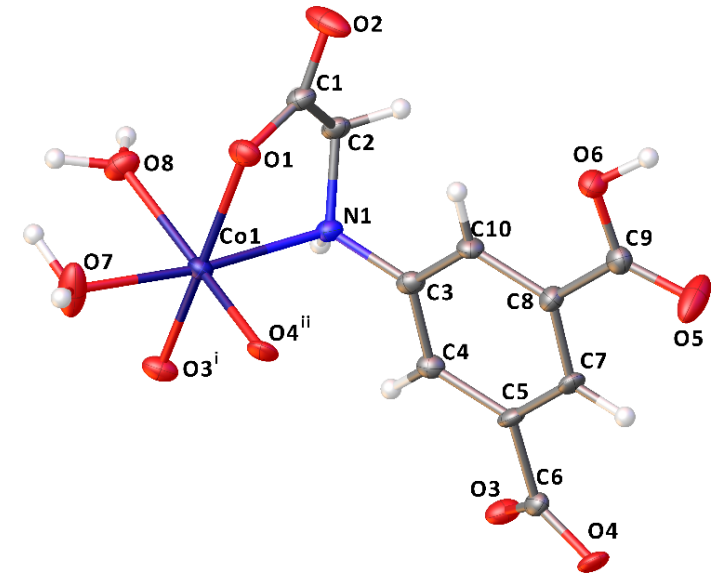


**Figure S39.** The asymmetric unit of compound **9** and coordination sphere of Co1. (i, 2 – *x*, – 1/2 + *y*, 1 – *z*; ii, 1 – *x*, – 1/2 + *y*, 1 – *z*).

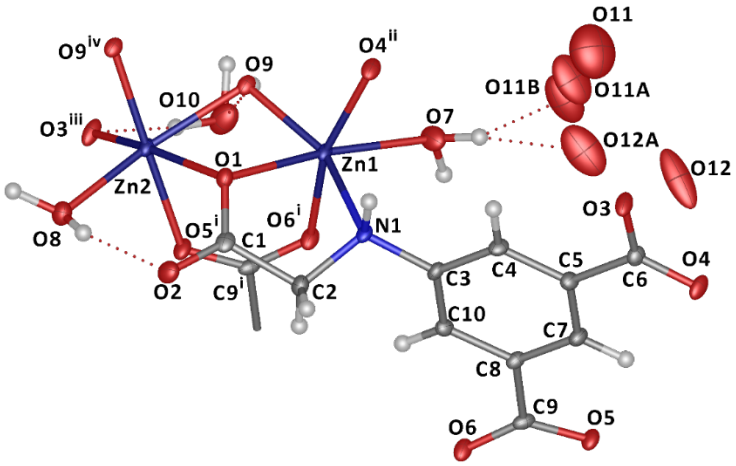


**Figure S40.** The asymmetric unit of compound **10** and the coordination spheres of Zn1 and Zn2. (i, 1 – *x*, 1 – *y*, – *z*; ii, 1/2 + *x*, 3/2 – *y*, 1/2 + *z*; iii, 3/2 – *x*, – 1/2 + *y*, 1/2 – *z*; iv, 2 – *x*, 1 – *y*, 1 – *z*).

## 4. Void space analyses

Void spaces in compounds **3**, **5**, **6** and **10** are shown in Figures S41-S44 respectively.

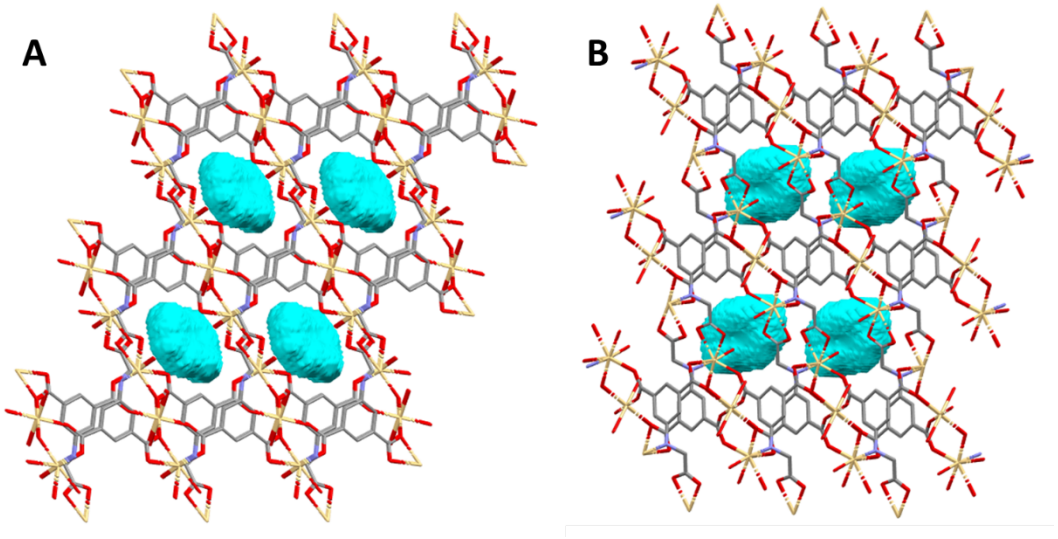


**Figure S41.** The void space in compound **3** as viewed down the **A.** *a*-axis and **B**. *b*-axis. (Cd = yellow, O = red, N = blue, C = grey, H = removed for clarity, Void space = cyan).

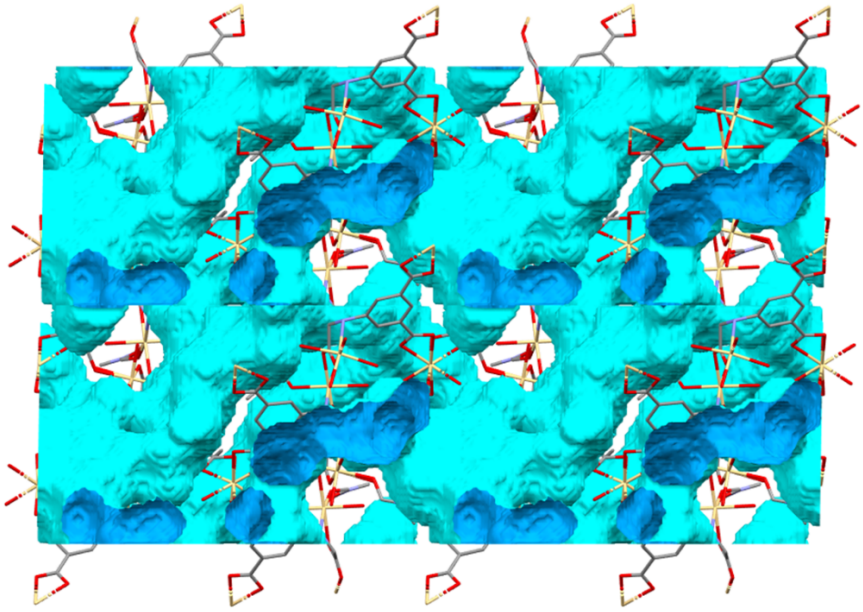

**Figure S42.** The void space in compound **5** viewed down the *b*-axis. (Void space exterior = Cyan, Void space interior = blue).

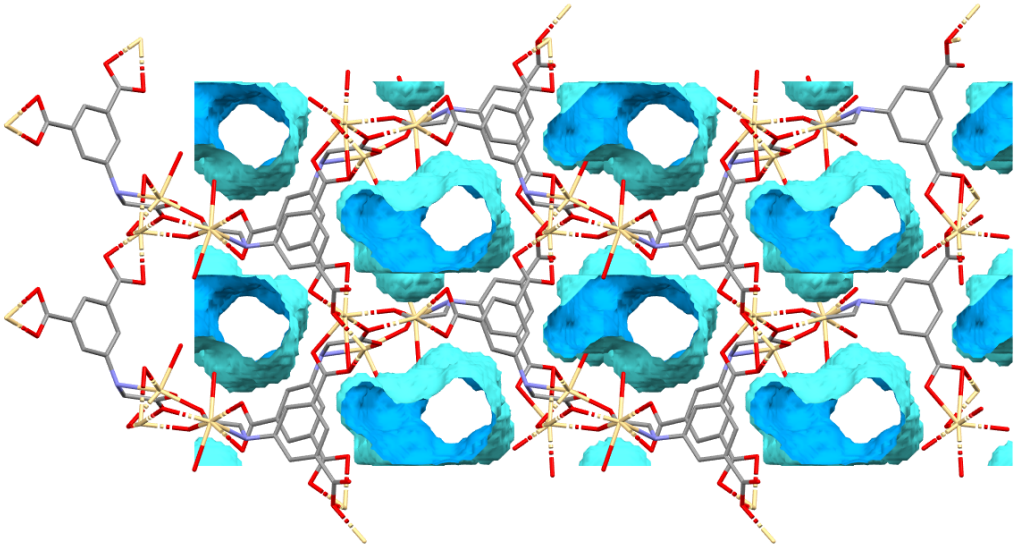

**Figure S43.** The void space in compound **6** viewed down the *c*-axis. (Void space exterior = Cyan, Void space interior = blue).

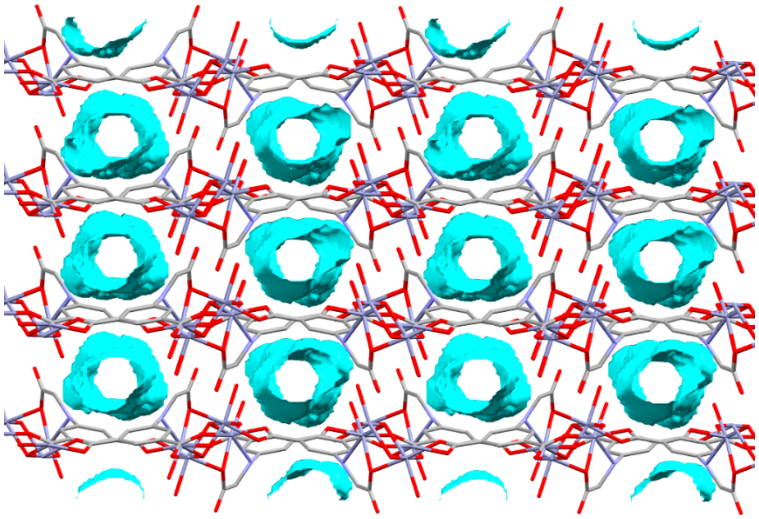

**Figure S44.** The void space in compound **10**.

## 5. References


S1. G. Sheldrick, *Acta Crystallogr. Sect. C*, 2015, **71**, 3-8.

S2. O. V. Dolomanov, L. J. Boulhis, R. J. Gildea, J. A. K. Howard and H. Puschmann, *J. Appl. Cryst.*, 2009, **42**, 339-341.